Editors' Suggestion

Quantum kinetic theory for quantum electrodynamics

Shu Lin *

School of Physics and Astronomy, Sun Yat-Sen University, Zhuhai 519082, China

(Received 10 January 2022; accepted 22 March 2022; published 22 April 2022)

We derive a quantum kinetic theory for QED based on Kadanoff-Baym equations for Wigner functions. By assuming parity invariance and considering a complete set of self-energy diagrams, we find that the resulting kinetic theory expanded to lowest order in $\hbar$ generalizes the well-known classical kinetic theory to the massive case. It contains elastic and inelastic collision terms and integrates a screening effect naturally. For a given solution to the classical kinetic theory, we find at next order in $\hbar$ a nondynamical quantum correction to Wigner functions for both fermions and photons, which gives rise to spin polarization for fermions and photons, respectively. The approach allows us to study the nondynamical part of the collisional effect on the spin polarization phenomenon.

DOI: 10.1103/PhysRevD.105.076017

I. INTRODUCTION AND SUMMARY

Spin polarization phenomena have been observed in a variety of experiments in particle physics [1–3] and condensed matter physics [4,5]. It can be induced by different sources such as electromagnetic field [6,7] and vorticity [8–11]. In order to describe spin transports in a nonequilibrium setting, two complementary frameworks have been developed. One is spin kinetic theory [12–16], which generalizes the chiral kinetic theory [17–35] to the massive case. Spin kinetic theory is organized as a systematic expansion in $\hbar$, where the zeroth order gives the classical kinetic theory, and the spin effect appears from the first order. Recently, much progress has been made toward realistic collision terms for spin kinetic theory [22,36–47]. However a complete derivation of the realistic collision term for QCD has yet to be performed.

The other framework is spin hydrodynamics [48–60], which includes spin density as an additional degree of freedom in conventional hydrodynamics. It is assumed that the spin density relaxes much slower than the other nonhydrodynamic modes. The assumption clearly depends on particular microscopic theory. It is desirable to confirm that such an assumption is indeed satisfied in systems of our interest.

In this paper, we derive quantum kinetic equations for quantum electrodynamics (QED) based on Kadanoff-Baym (KB) equations. This approach allows us to incorporate complete collision term for fermions and photons. By performing an expansion in $\hbar$ of the resulting kinetic equations, we obtain at the lowest order a classical kinetic theory. On general grounds, one expects classical kinetic theory to agree with the classical Boltzmann equations written by Arnold, Moore, and Yaffe (AMY) [61–63] for quantum chromodynamics (QCD), which is essentially spin-averaged kinetic equations. The agreement is achieved by assumption of parity invariance. It is known that for massive fermions, the kinetic theory contains the following degrees of freedom: f_V^e/f_A^e and a_μ, being vector/axial charge distribution functions and spin direction, respectively [12]. By assuming the system is parity invariant, we are left with f_V^e (to be denoted as f_e) as the only degree of freedom. A similar reduction applies to the photonic sector of kinetic theory, leaving only the distribution function of unpolarized photon f_γ as the degree of freedom. With these simplifications, we find the resulting classical kinetic theory generalizes the classical Boltzmann equation by AMY [61–63] to the massive case for QED. The generalization to the massive case is crucial for the phenomenology of spin polarization.

The classical kinetic equation serves as a background on which we can study quantum correction by systematic expansion in $\hbar$ within our approach. As we show in Sec. V, the quantum correction at next order gives rise to spin polarization of both fermions and photons. Our approach bridges the gap between realistic classic kinetic theory and formal development of quantum kinetic theory, thus allowing us to study the collisional contribution to spin polarization phenomena in a realistic system. It is also worth mentioning that in early studies of transport coefficients in classical kinetic theory [61–63] gradient expansion is employed, while $\hbar$ is set to unity. In fact, we clarify the relation between two expansions in Sec. V. From our

*linshu8@mail.sysu.edu.cn

approach, it is manifest that gradient expansion in classical kinetic theory already includes a partial contribution of $\hbar$ expansion, which does not lead to spin polarization. We still use the terminology of classical and quantum kinetic theory as a separation between spin unpolarized and polarized sectors of the kinetic theory.

It is informative to compare the classical kinetic theories for QED and QCD. On one hand, they share similar scales: characteristic momentum of quasiparticles Λ, thermal/screening mass $e\Lambda(g\Lambda)$, and damping rate of quasiparticles $e^2\Lambda(g^2\Lambda)$. One the other hand, they differ in one fundamental aspect: QED does not possess a nonpertubative scale, while QCD does. The nonperturbative scale for QCD cuts off long range fluctuation of chromoelectromagnetic fields, allowing for omission fluctuation of chromoelectromagnetic fields beyond the scale $\frac{1}{g^2\Lambda}$. However, such a mechanism is not present in QED. We instead choose a larger coarse-graining scale $\frac{1}{e^4\Lambda}$ for the kinetic theory and restrict ourselves to the situation without background electromagnetic fields. We show that electromagnetic fields generated by fluctuations at the scale $\frac{1}{e^4\Lambda}$ have a subleading effect as compared to that of spacetime gradients.

The paper is organized as follows: in Sec. II, we derive the Kadanoff-Baym equations for fermions and photons. By the assumption of parity invariance, the degrees of freedom are identified as unpolarized fermion/photon distribution functions. We also discuss regimes of validity of the kinetic theory. In Secs. III and IV, we elaborate on the self-energies of fermions and photons, which gives rise to the elastic and inelastic collision terms. In order to incorporate the interference term in the $2 \leftrightarrow 2$ process and $1 \leftrightarrow 2$ process, it is crucial to include vertex correction in the self-energies. The resulting kinetic equations to lowest order in $\hbar$ show a clear resemblance to the Boltzmann equations by AMY. In Sec. V, we consider the next order expansion in $\hbar$. After enumerating possible $\hbar$ corrections, we focus on a nondynamical type of correction, which gives rise to spin polarization and is entirely fixed by solution of the classical kinetic equation. We provide an outlook in Sec. IV.

II. KADANOFF-BAYM EQUATIONS FOR QED

A. Fermionic Kadanoff-Baym equations

We begin by writing the fermionic part of the Lagrangian,

$$\frac{\mathcal{L}}{\hbar} = \bar{\psi}\left(i\partial\!\!\!/ - eA\!\!\!/ - \frac{m}{\hbar}\right)\psi + \bar{\eta}\psi + \bar{\psi}\eta, \tag{1}$$

where $\bar{\eta}$ and η are sources coupled to ψ and $\overline{\psi}$, respectively. We first write the Dyson-Schwinger equation on the Schwinger-Keldysh (SK) contour,

$$\left(i\partial\!\!\!/_x - \frac{m}{\hbar}\right)\psi(x) = \eta(x) + \eta_{\rm ind}(x), \tag{2}$$

$$\bar{\psi}(y)\left(-i\overleftarrow{\partial\!\!\!/}_y - \frac{m}{\hbar}\right) = \bar{\eta}(y) + \bar{\eta}_{\rm ind}(y), \tag{3}$$

with $\eta_{\rm ind} = eA\!\!\!/\psi$ and $\bar{\eta}_{\rm ind} = e\bar{\psi}A\!\!\!/$.[1] For simplicity, we have assumed the absence of background gauge field. Following [64], we take the derivative $i\frac{\delta}{\delta\eta(y)}$ on (2) to obtain

$$\left(i\partial\!\!\!/_x - \frac{m}{\hbar}\right)S_c(x,y) = i\delta_c(x-y) + i\frac{\eta_{\rm ind}(x)}{\eta(y)}, \tag{4}$$

where the subscript indicates the quantity being contour-time ordered. The matrix form of $S_c(x,y)$ in 12 basis is given by

$$\begin{aligned} S_{c,\alpha\beta}(x,y) &= \begin{pmatrix} S^{11}_{\alpha\beta}(x,y) & S^{<}_{\alpha\beta}(x,y) \\ S^{>}_{\alpha\beta}(x,y) & S^{22}_{\alpha\beta}(x,y) \end{pmatrix} \\ &= \begin{pmatrix} \langle T\psi_\alpha(x)\bar{\psi}_\beta(y)\rangle & -\langle\bar{\psi}_\beta(y)\psi_\alpha(x)\rangle \\ \langle\psi_\alpha(x)\bar{\psi}_\beta(y)\rangle & \langle\bar{T}\psi_\alpha(x)\bar{\psi}_\beta(y)\rangle \end{pmatrix}. \end{aligned} \tag{5}$$

We have also kept explicit Dirac indices $\alpha\beta$ in (5). T and $\bar{T}$ correspond to time ordering and antitime ordering. The last term of (4) can be evaluated as

$$\begin{aligned} \frac{\delta}{\delta\eta(y)}\eta_{\rm ind}(x) &= \int d^4z\left(-i\frac{\delta}{\delta\psi(z)}\eta_{\rm ind}(x)\right)\left(i\frac{\delta}{\delta\eta(y)}\delta\psi(z)\right) \\ &= \int d^4z\Sigma_c(x,z)S_c(z,y), \end{aligned} \tag{6}$$

with $\Sigma_c(x,y) = -i\frac{\delta}{\delta\psi(y)}\eta_{\rm ind}(x) = \langle\eta_{\rm ind}(x)\bar{\eta}_{\rm ind}(y)\rangle_c$. Taking x and y on the forward and backward contours, respectively, we obtain

$$\begin{aligned} \left(i\partial\!\!\!/_x - \frac{m}{\hbar}\right)S^<(x,y) &= i\int d^4z\Sigma_F(x,z)S^<(z,y) \\ &\quad - i\int d^4z\Sigma^<(x,z)S_{\bar{F}}(z,y). \end{aligned} \tag{7}$$

We can eliminate the time ordered self-energy Σ_F and antitime ordered correlator $S_{\bar{F}}$ in favor of a retarded/advanced correlator defined as

$$S_R(x,y) = i\theta(x_0-y_0)(S^>(x,y) - S^<(x,y)),$$
$$S_A(x,y) = -i\theta(y_0-x_0)(S^>(x,y) - S^<(x,y)),$$

and similar definitions for $\Sigma_{R/A}$. Using the following relations:

[1] Recall the dimensions of fields: $\psi \sim \text{length}^{-3/2}$, $A \sim \text{length}^{-1}$. By writing the vertex in (1), we have redefined the coupling constant e such that it contains no factor of $\hbar$.

$$\Sigma_F(x,z) = -i\Sigma_R(x,z) + \Sigma^<(x,z),$$
$$S_{\bar{F}}(z,y) = S^<(z,y) + iS_A(z,y), \tag{8}$$

we arrive at the standard form of KB equations for fermions,

$$\left(i\partial\!\!\!/_x - \frac{m}{\hbar}\right)S^<(x,y) = \int d^4z(\Sigma_R(x,z)S^<(z,y) + \Sigma^<(x,z)S_A(z,y)). \tag{9}$$

We rewrite (9) in terms of a Wigner transformed lesser propagator,

$$\tilde{S}^<\left(X = \frac{x+y}{2}, P\right) = \int d^4(x-y)e^{iP\cdot(x-y)/\hbar}\langle S^<(x,y)\rangle. \tag{10}$$

The rhs can be expressed using $\tilde{S}^<(X,P)$ and the counterpart for self-energy by the following expansion:

$$\int d^4zA(x,z)B(z,y) = \int_K e^{-iK\cdot(x-y)}\left(\tilde{A}\,\tilde{B} + \frac{i\hbar}{2}\{\tilde{A},\tilde{B}\}_{\rm PB}\right) + O(\hbar^2), \tag{11}$$

where the Poisson bracket is defined as

$$\{\tilde{A},\tilde{B}\} = \partial_k\tilde{A}\cdot\partial_X\tilde{B} - \partial_X\tilde{A}\cdot\partial_k\tilde{B}, \tag{12}$$

and $\int_K \equiv \int \frac{d^4K}{(2\pi)^4}$. The Wigner transform of (9) then reads

$$\frac{i}{2}\partial\!\!\!/ S^< + \frac{P\!\!\!/ - m}{\hbar}S^< = (\Sigma_R S^< + \Sigma^< S_A) + \frac{i\hbar}{2}(\{\Sigma_R, S^<\}_{\rm PB} + \{\Sigma^<, S_A\}_{\rm PB}). \tag{13}$$

We have dropped the tildes and the common arguments (X,P) for propagators and self-energies for notational simplicity.

To proceed further, we use the quasiparticle approximation [64], in which the spectral density is given by

$$\rho(X,P) = S^>(X,P) - S^<(X,P) = 2\pi\hbar\epsilon(p_0)(P\!\!\!/ + m)\delta(P^2 - m^2 - 2P^\mu{\rm Re}\Sigma^R_\mu), \tag{14}$$

where $\epsilon(p_0)$ is the sign function, and $\Sigma^R_\mu = \frac{1}{4}{\rm tr}[\gamma_\mu\Sigma^R]$. The structure of (14) indicates that the quasiparticle has a momentum shifted by ${\rm Re}\Sigma^R_\mu$ and has a vanishing damping rate $\Gamma(X,P)$. For a system with characteristic momenta Λ, ${\rm Re}\Sigma^R \sim e\Lambda$ and damping rate $\sim e^2\Lambda$. We can indeed ignore ${\rm Re}\Sigma^R_\mu$ next to P_μ and Γ. We can use the following representations to further simplify (13)[2]:

$$\Sigma^R = {\rm Re}\Sigma^R + \frac{i}{2}(\Sigma^> - \Sigma^<),$$
$$S^A = {\rm Re}S^R - \frac{i}{2}(S^> - S^<),$$

and ignore ${\rm Re}\Sigma^R$ and ${\rm Re}S^R \propto \Gamma$ as reasoned above to arrive at

$$\frac{i}{2}\partial\!\!\!/ S^< + \frac{P\!\!\!/ - m}{\hbar}S^< = \frac{i}{2}(\Sigma^> S^< - \Sigma^< S^>) - \frac{\hbar}{4}(\{\Sigma^>, S^<\}_{\rm PB} - \{\Sigma^<, S^>\}_{\rm PB}). \tag{15}$$

Equation (15) can be solved order by order in $\hbar$,

$$S^< = S^{<(0)} + \hbar S^{<(1)} + \hbar^2 S^{<(2)} + \cdots, \tag{16}$$

with the lowest order solution given by [12],[3]

$$S^{<(0)} = -2\pi\hbar\epsilon(P\cdot u)\delta(P^2 - m^2)\left((P\!\!\!/ + m)f^e_V + \gamma^5 a\!\!\!/ f^e_A - \frac{\sigma^{\mu\nu}}{2}\frac{\epsilon_{\mu\nu\rho\sigma}P^\rho a^\sigma}{m}f^e_A\right). \tag{17}$$

Note that we have introduced an observer's frame vector u in the sign function, which separates particles and antiparticles. Despite the appearance of u, it is actually frame independent at this order because boosts do not change a particle into antiparticle. f^e_V/f^e_A and a^μ correspond to vector/axial distributions and spin direction vectors, respectively. We assume that the system is parity invariant, which means $f^e_A = 0$, leaving f^e_V as the only degree of freedom.[4] This is identified as a fermion distribution function in classical kinetic theory. We denote f^e_V as f_e below. The lowest order solution can be written as

$$S^{<(0)}(X,P) = -2\pi\hbar\epsilon(P\cdot u)\delta(P^2 - m^2)(P\!\!\!/ + m) \times f_e(X,P), \tag{18}$$

which is nothing but the equilibrium fermion propagator with Fermi-Dirac distribution promoted to spacetime-dependent distribution f_e.

[2]The real part is formally defined with a Hermitian conjugate as ${\rm Re}A = \frac{1}{2}(A + \gamma^0 A^\dagger \gamma^0)$.

[3]The overall factor of $\hbar$ can be removed by a redefinition of the Wigner function. We give a more detailed account of the formal expansion in Sec. V.

[4]It is parity invariant in the sense that there is no difference between distributions of opposite chiral components and similarly for photons. However, in an out-of-equilibrium setting, parity can be broken by sources, such as spacetime gradient of temperature and fluid velocity, etc.

In fact, f_e satisfies the constraint $f_e(X,P)+f_e(X,-P)=1$, like a Fermi-Dirac distribution. To see the origin of the constraint, we can show from the definition (5) that $\mathrm{tr}[S^<(x,y)] = -\mathrm{tr}[S^>(y,x)]$, which gives $\mathrm{tr}[S^<(X,P)] = -\mathrm{tr}[S^>(X,-P)]$. Combining with (18), we easily arrive at the constraint. Furthermore, we have the following property:

$$S^{>(0)}(X,-P,m) = S^{<(0)}(X,P,-m). \tag{19}$$

Defining

$$\bar{S}^{>/<(0)}(X,P,m) = S^{>/<(0)}(X,P,-m), \tag{20}$$

we can then write the following useful relations:

$$\bar{S}^{<(0)}(X,P,m) = S^{>(0)}(X,-P,m), \tag{21}$$

and a similar one with $> \leftrightarrow <$. Below, S and $\bar{S}$ always contain the argument m, which we omit from now. Equation (21) suggests the interpretation of $\bar{S}^{>/<(0)}$ as a charge-conjugated Wigner function. To arrive at the classical kinetic theory, we always deal with fermions with positive energy. For $P\cdot u > 0$, we use $S^{<(0)}(X,P)$ to describes particles, while for $P\cdot u < 0$, we use $\bar{S}^{>(0)}(X,-P)$ instead to switch to an antiparticle description.

B. Photonic Kadanoff-Baym equations

We now turn to the photonic counterpart starting with the following relevant part of the Lagrangian:

$$\frac{\mathcal{L}}{\hbar} = -\frac{1}{4}F_{\mu\nu}^2 + \bar{\psi}(-e\slashed{A}_\mu)\psi - A_\mu j^\mu - \frac{1}{2\xi}(P^{\alpha\beta}\partial_\alpha A_\beta)^2, \tag{22}$$

where j^μ is the source to A_μ. The last term is the gauge fixing term for Coulomb gauge, with the projector $P^{\alpha\beta}$ defined with an observer's frame vector n^α as $P^{\alpha\beta} = n^\alpha n^\beta - g^{\alpha\beta}$. We take n^μ to be the same frame vector as the fermionic one u^μ. It projects out the temporal component of a vector. The Coulomb gauge singles out a transversely polarized photon as the physical degrees of freedom, offering a quick path to kinetic theory.

The Dyson-Schwinger equation for a photon is given by

$$\begin{aligned}(\partial^2 g^{\mu\nu} - \partial^\mu\partial^\nu)A_\nu(x) + \frac{1}{\xi}(P^{\mu\nu}\partial_\nu P^{\alpha\beta}\partial_\alpha A_\beta(x))\\ = j^\mu(x) + j^\mu_{\mathrm{ind}}(x),\end{aligned} \tag{23}$$

where $j^\mu_{\mathrm{ind}} = \bar{\psi}\gamma^\mu\psi$. Taking the derivative $i\frac{\delta}{\delta j^\rho(y)}$ on the SK-contour, we obtain

$$\begin{aligned}\left(\partial^2 g^{\mu\nu} - \partial^\mu\partial^\nu + \frac{1}{\xi}P^{\mu\alpha}P^{\nu\beta}\partial_\alpha\partial_\beta\right)_x D^c_{\nu\rho}(x,y)\\ = i\delta^\mu_\rho\delta_c(x-y) + i\int d^4z\,\Pi^{\mu\nu}_c(x,z)D^c_{\nu\rho}(z,y),\end{aligned} \tag{24}$$

where $D^c_{\nu\rho}(x,y) = \langle A_\nu(x)A_\rho(y)\rangle_c$ and $\Pi^{\mu\nu}_c(x,y) = \langle j^\mu_{\mathrm{ind}}(x)j^\nu_{\mathrm{ind}}(y)\rangle_c$. The subscript x indicates the derivatives acting on x. The usual Coulomb gauge is recovered in the limit $\xi \to 0$,

$$P^{\mu\alpha}\partial^x_\alpha D^<_{\mu\nu}(x,y) = 0. \tag{25}$$

Following similar procedures as the fermionic case for the Wigner transform and quasiparticle approximation, we arrive at

$$\begin{aligned}&\left[\frac{1}{\hbar^2}\left(-P^2 g^{\mu\nu} + P^\mu P^\nu - \frac{1}{\xi}P^{\mu\alpha}P^{\nu\beta}P_\alpha P_\beta\right) + \frac{i}{2\hbar}\left(-2P\cdot\partial g^{\mu\nu} + (\partial^\mu P^\nu + \partial^\nu P^\mu) - \frac{1}{\xi}P^{\mu\alpha}P^{\nu\beta}(\partial_\alpha P_\beta + \partial_\beta P_\alpha)\right)\right.\\ &\left.+\frac{1}{4}\left(\partial^2 g^{\mu\nu} - \partial^\mu\partial^\nu + \frac{1}{4\xi}P^{\mu\alpha}P^{\nu\beta}\partial_\alpha\partial_\beta\right)\right]D^<_{\nu\rho} = \frac{i}{2}(\Pi^{\mu\nu>}D^<_{\nu\rho} - \Pi^{\mu\nu<}D^>_{\nu\rho}) + \frac{\hbar}{4}\{\Pi^{\mu\nu>}, D^<_{\nu\rho}\} - \frac{\hbar}{4}\{\Pi^{\mu\nu<}, D^>_{\nu\rho}\},\end{aligned} \tag{26}$$

with the Coulomb gauge condition,

$$P^{\mu\alpha}\left(\frac{\hbar}{2}\partial_\alpha - iP_\alpha\right)D^<_{\mu\nu} = 0. \tag{27}$$

We seek solutions to (26) and (27) order by order in $\hbar$,

$$D^<_{\mu\nu} = D^{<(0)}_{\mu\nu} + \hbar D^{<(1)}_{\mu\nu} + \cdots, \tag{28}$$

with the lowest order solution given by [65–67]

$$D^{<(0)}_{\mu\nu} = 2\pi\hbar^2\epsilon(P\cdot u)\delta(P^2)(P^T_{\mu\nu}f^\gamma_V - iS_{\mu\nu}f^\gamma_A), \tag{29}$$

where $P^T_{\mu\nu} = P_{\mu\nu} - \frac{P_{\mu\alpha}P_{\nu\beta}P^\alpha P^\beta}{-P^2+(P\cdot u)^2}$ and $S_{\mu\nu} = \frac{\epsilon_{\mu\nu\rho\sigma}P^\rho u^\sigma}{P\cdot u}$ are parity even and odd projectors perpendicular to $P_{\mu\alpha}P^\alpha$, respectively. With these projectors, the Coulomb gauge condition (27) is automatically satisfied. Similar to the fermionic case, in a parity invariant system, $f^\gamma_A = 0$, and we denote f^γ_V as f_γ, which is to be identified as a photon distribution function. We have then a simplified the Wigner function for photons,

$$D^{<(0)}_{\mu\nu}(X,P) = 2\pi\hbar^2\epsilon(P\cdot u)\delta(P^2)P^T_{\mu\nu}f_\gamma(X,P), \tag{30}$$

which is nothing but the equilibrium photon propagator in Coulomb gauge with Bose-Einstein distribution promoted to spacetime-dependent distribution f_γ. Similar to the fermionic case, the distribution satisfies the constraint $f_\gamma(X,-P) = -1 - f_\gamma(X,P)$. It follows from

$$D^{<}_{\mu\nu}(x,y) = D^{>}_{\nu\mu}(y,x)$$
$$\Rightarrow D^{<(0)}_{\mu\nu}(X,P) = D^{>(0)}_{\nu\mu}(X,-P) = D^{>(0)}_{\mu\nu}(X,-P), \quad (31)$$

upon using (30).

C. Classical kinetic equations and regime of validity

Now we determine the dynamics of f_e and f_γ. For the former, it is known that $S^{<(1)}$ contains only axial and tensor components [12,39]. Taking the trace of (15), we find $\mathrm{tr}[(\not{P}-m)S^{<(1)}] = 0$, and we arrive at

$$\mathrm{tr}[\not{\partial}S^{<(0)}] = \mathrm{tr}[\Sigma^{>(0)}S^{<(0)} - \Sigma^{<(0)}S^{>(0)}], \quad (32)$$

where $S^{<(0)}$ is given by (18).

For the latter, we assume $D^{<(1)}_{\nu\rho}$ is on shell. The dynamics of f_γ can be derived by contracting (26) with $P^{T,\rho}_\mu$. We find $P^{T,\rho}_\mu(-P^2 g^{\mu\nu} + P^\mu P^\nu - \frac{1}{\xi}P^{\mu\alpha}P^{\nu\beta}P_\alpha P_\beta)D^{<(1)}_{\nu\rho} = 0$ at $O(\hbar^{-1})$. The remaining terms give the dynamical equation for f_γ,

$$-2P\cdot\partial g^{\mu\nu}D^{<(0)}_{\nu\mu} = \hbar(\Pi^{\mu\nu>(0)}D^{<(0)}_{\nu\mu} - \Pi^{\mu\nu<(0)}D^{>(0)}_{\nu\mu}). \quad (33)$$

The presence of $\hbar$ in the classical kinetic equation is consistent with the dimension of photon self-energies $\Pi^{\mu\nu>/<}(X,P) \sim \text{length}^{-2}$.

Let us express the lhs of (32) and (33) in terms of distributions f_e and f_γ. Taking $p_0 > 0$, we have

$$\begin{aligned}\mathrm{tr}[\not{\partial}S^{<(0)}(X,P)] &= (-2\pi\hbar)4P\cdot\partial\delta(P^2-m^2)f_e(X,P)\\ &= (-2\pi\hbar)\frac{2}{E_p}P\cdot\partial f_e(X,P)\delta(p_0-E_p),\\ -2P\cdot\partial g^{\mu\nu}D^{<(0)}_{\nu\mu}(X,P) &= (2\pi\hbar^2)4P\cdot\partial\delta(P^2)f_\gamma(X,P)\\ &= (2\pi\hbar^2)\frac{2}{p}P\cdot\partial f_\gamma(X,P)\delta(p_0-p),\end{aligned} \quad (34)$$

with $E_p = (p^2+m^2)^{1/2}$. Dividing out the xfactor 2 converts the spin-summed collision term to the spin-averaged one for either fermions or photons. We have only kept the particle contributions in (34). The kinetic equation for antiparticles can be obtained from the corresponding equations for $S^{<(0)}(X,-P)$ and $D^{<(0)}_{\nu\rho}(X,-P)$. Note that photon is its own antiparticle, so the resulting equation is expected to be equivalent. For fermions, we obtain

$$\begin{aligned}\mathrm{tr}[\not{\partial}S^{<(0)}(X,-P)] &= (2\pi\hbar)4P\cdot\partial\delta(P^2-m^2)f_e(X,-P)\\ &= (-2\pi\hbar)\frac{2}{E_p}P\cdot\partial f_{\bar{e}}(X,P)\delta(p_0-E_p),\end{aligned} \quad (35)$$

with $f_{\bar{e}}(X,P) \equiv 1 - f_e(X,-P)$ identified as a distribution function for antiparticles. Note that $f_e(X,P)$, $f_{\bar{e}}(X,P)$, and $f_\gamma(X,P)$ all have positive energies, so we may also denote them as $f_e(X,\vec{p})$, $f_{\bar{e}}(X,\vec{p})$ and $f_\gamma(X,\vec{p})$.

In order to close the equations, we need to express $\Sigma^{</>(0)}$ and $\Pi^{\mu\nu>/<(0)}$ on the rhs of (32) and (33) in terms of f_e and f_γ as well. This is the subject of the next two sections. As we see, the self-energies consistently incorporate elastic and inelastic collisions in the known classical kinetic theory. The final expressions for the elastic and inelastic contributions can be found in (49), (50) and (102), (88) respectively. We set $\hbar = 1$ in the next two sections, with the understanding that factors of $\hbar$ can always be reinstated by dimension in the classical collision term. We retain $\hbar$ in Sec. V when we discuss quantum corrections.

Before presenting details on the self-energies, we discuss the regime of validity of the kinetic theory. The key conditions to be satisfied are the following:

- (i) There is a separation of scales between quasiparticle momenta Λ, thermal mass $e\Lambda$, and damping rate $e^2\Lambda$.
- (ii) The physical observable of our interest is dominated by the dynamics of quasiparticles, which are described by the kinetic theory.
- (iii) The coordinate in the kinetic theory is coarse grained within the scale $1/e^4\Lambda$. Collisions are local on every coarse-grained spacetime point. The coarse-graining scale is also crucial for condition v below.
- (iv) The distributions can only be weakly anisotropic such that instability associated with electromagnetic fields does not affect the dynamics of quasiparticles.
- (v) A background electromagnetic field is excluded by assumption. The effect of electromagnetic fields from thermal fluctuations is also neglected compared to spacetime derivatives of distributions $e|A| \ll \partial_X f/f$. This is possible if we assume $e^6\Lambda \ll \partial_X f/f \lesssim e^4\Lambda$. As we show below, the large conductivity of the medium suppresses the fluctuation of electromagnetic fields $e|A| \sim e^6\Lambda$ so that our assumption on the gradient of distribution always dominates over electromagnetic fields from fluctuations.
- (vi) Since the equations and solutions are organized by expansion in $\hbar$, we need to have the quantum correction small compared to the classical counterpart. This is guaranteed by $\hbar\partial_X f \ll \Lambda$.

We do not elaborate on iv through vi below:

- (iv) It is known that an anisotropic distribution in momentum can lead to filamentation instability, in which electromagnetic field draws energy from quasiparticles and grows exponentially [68], see Ref. [69] for a recent review. The scale of the instability can be estimated following [70]. For a given class of anisotropic distributions $f_{\rm iso}(\sqrt{\mathbf{p}^2+\xi(\mathbf{p}\cdot\mathbf{n})^2})$, with ξ and n corresponding to magnitude and axis of anisotropy respectively, the unstable modes for a weakly anisotropic case $\xi \ll 1$ is found to have a characteristic frequency $\xi^{3/2}e^2T$ [70]. In order for the unstable mode not to invalidate the kinetic theory, we require that the instability occurs more slowly than the characteristic timescale of the kinetic theory $\xi^{3/2}e^2T \ll e^4T$, which leads to $\xi^{3/2} \ll e^2$.

(v) Now we justify the omission of electromagnetic fields. While we exclude background electromagnetic fields by assumption, the latter can still be generated by thermal fluctuations. We show that their effect is subleading compared to that of spacetime derivatives. The magnitude of the fluctuation depends on the property of the medium and the timescale of the fluctuation. For simplicity, we probe the medium in equilibrium, which is expected to give the correct parametric estimate. We probe the medium with an external current $(\rho_{\rm ex}, \vec{j}_{\rm ex})$. The electromagnetic fields satisfy Maxwell equations,

$$\nabla\times\vec{E} = -\partial_t\vec{B}, \qquad \nabla\cdot\vec{B} = 0,$$
$$\nabla\times\vec{H} = \vec{j}_{\rm ex} + \partial_t\vec{D}, \qquad \nabla\cdot\vec{D} = \rho_{\rm ex}. \tag{36}$$

The difference between $\vec{H}$ and $\vec{B}$ is supposed to come from the spin of charge carriers, which comes from next order in $\hbar$, so we ignore them. The electric displacement and electric field are related by $\vec{D} = \epsilon\vec{E}$, with ϵ being the dielectric constant characterizing the property of the medium. We may solve $\vec{E}$ in momentum space as

$$i\frac{\vec{q}\times(\vec{q}\times\vec{E})}{q_0} = \vec{j}_{\rm ex} - iq_0\epsilon\vec{E}. \tag{37}$$

Equation (37) encodes the response of $\vec{E}$ to $\vec{j}_{\rm ex}$. In the gauge $A_0 = 0$, (37) gives rise to the following retarded correlator:

$$\langle A_i(q_0,\vec{q})A_i(q_0',\vec{q}')\rangle_R \sim \frac{1}{q_0^2\epsilon - q^2}\delta(q_0+q_0')\delta^3(\vec{q}+\vec{q}') \quad \vec{q}\perp\vec{A},$$
$$\langle A_i(q_0,\vec{q})A_i(q_0',\vec{q}')\rangle_R \sim \frac{1}{q_0^2\epsilon}\delta(q_0+q_0')\delta^3(\vec{q}+\vec{q}') \quad \vec{q}\parallel\vec{A}. \tag{38}$$

On the coarse-graining scale of the coordinate, the medium is known to be a very good conductor, so that we can parametrize the dielectric constant as

$$\epsilon \simeq 1 + \frac{i\sigma}{q_0}, \tag{39}$$

with $\sigma \sim \frac{T}{e^2}$ [62,63]. For the purpose of a parametric estimation, we regard $q \sim q_0$ and not distinguish between longitudinal and transverse cases in (38). The retarded correlator in (38) dictates the symmetrized correlator of electromagnetic fields by the fluctuation-dissipation theorem [71],

$$\begin{aligned}\langle A_i(q_0,\vec{q})A_i(q_0',\vec{q}')\rangle_{\rm sym} &= \frac{2T}{q_0}{\rm Im}\langle A_i(q_0,\vec{q})A_i(q_0',\vec{q}')\rangle_R \\ &\sim \frac{T}{q_0}{\rm Im}\frac{1}{q_0^2+i\sigma q_0}\delta(q_0+q_0')\delta^3(\vec{q}+\vec{q}').\end{aligned} \tag{40}$$

Noting that $\sigma \gg q_0$, we obtain the following estimate for fluctuation of electromagnetic gauge fields in coordinate space:

$$|A_i(t,x)| \sim \left(\frac{T}{q_0^2\sigma}q_0q^3\right)^{1/2} \sim e^5T, \tag{41}$$

where we have Fourier transformed to coordinate space and taken $q_0 \sim q \sim e^4T$ since we are concerned with the fluctuation of the electromagnetic field over the coarse-graining distance. It follows that the effect of fluctuating electromagnetic fields can be ignored because the spacetime derivatives are much larger than the mean fluctuation of electromagnetic fields $e^4T \gtrsim \partial_X f/f \gg e|A_i| \sim e^6T$ by our assumption. The origin of the small fluctuation can be attributed to large conductivity, which disfavors fluctuation of electromagnetic fields.

While the electromagnetic field can be neglected over the coarse-graining scale, it does play a role within the scale $1/e\Lambda$ in the form of exchanged virtual photons in fermion scatterings. The corresponding resummed propagator for a virtual photon is fully determined by the distribution of real fermions in kinetic theory, see details at the end of Sec. III. Similarly, the virtual fermion relevant for scattering between a real fermion and photon is also fully determined by the on-shell degree of freedoms in the kinetic theory.

(vi) For the $\hbar$ expansion to be valid, we require the quantum correction to be small. We obtain in Sec. V that $\hbar S^{<(1)} \sim \hbar^2\partial_X f$, which is to be compared with $S^{<(0)} \sim \hbar\Lambda f$. This condition is clearly satisfied by

$\hbar\partial_X f \ll \Lambda$; i.e., the spacetime gradient needs to be small enough.

III. ELASTIC COLLISIONS

We begin with the $2 \to 2$ elastic collisions. These can be obtained from two-loop contributions to self-energies. As we see, there are both corrections to propagators and vertices. The former gives squares of amplitude in separate channels, and the latter gives interference terms between different channels.

In this section and the next one, we work solely with zeroth order quantities: $S^{</>(0)}$, $\Sigma^{</>(0)}$, $D_{\nu\rho}^{</>(0)}$, $\Pi^{\mu\nu</>(0)}$. To ease notations, we suppress the superscript (0).

A. Propagator corrections

To be specific, we focus on the term $\Sigma^>(P)S^<(P)$. $\Sigma^>$ has the following representation:

$$\Sigma^>(P) = e^2 \int_K \gamma^\mu S^>(K+P)\gamma^\nu D_{\nu\mu}^<(K). \qquad (42)$$

Since P is on shell, we cannot have both fermion momentum and photon momentum in the loop on shell. Indeed, the one-loop contribution does not capture dissipation effects, for which two-loop diagrams are needed. The two-loop diagrams containing propagator corrections are shown in Fig. 1, in which the left/right diagrams have one fermion/photon momentum off shell. Note that the 12 labels are uniquely determined by the requirement that three propagators attached to a vertex cannot be simultaneously on shell.

The left panel of Fig. 1 gives

$$\Sigma^>(P)S^<(P) = e^4 \int_{K,K'} \gamma^\mu S_{22}(K+P)\gamma^\rho S^>(P') \times \gamma^\sigma S_{11}(K+P)\gamma^\nu D_{\nu\mu}^<(K) D_{\rho\sigma}^>(K') S^<(P). \qquad (43)$$

$\Sigma^<(P)S^>(P)$ can be obtained from (43) by the replacements $> \leftrightarrow <$ and $1 \leftrightarrow 2$. The dependences of $S^{>/<}(P)$ on f_e suggest that $\Sigma^>(P)S^<(P)$ and $\Sigma^<(P)S^>(P)$ correspond to loss and gain terms, respectively. It is sufficient to focus on one term only. We show in the Appendix A that (43) gives rise to squares of s-channel Compton scattering, u-channel Compton scattering, and t-channel annihilation.

The right panel of Fig. 1 gives

$$\Sigma^>(P)S^<(P) = -e^4 \int_{P',K'} \gamma^\mu S^>(K)\gamma^\nu D_{\mu\beta}^{22}(P-K) \times D_{\alpha\nu}^{11}(P-K)\mathrm{tr}[\gamma^\alpha S^<(P')\gamma^\beta S^>(K')] \times S^<(P). \qquad (44)$$

Again, the replacements $> \leftrightarrow <$ and $1 \leftrightarrow 2$ in the above lead to $\Sigma^<(P)S^>(P)$. We show in Appendix A that (44) gives rise to squares of t-channel Coulomb scattering (between fermions), s-channel Coulomb scattering (between fermion and antifermion), and t-channel Coulomb scattering (between fermion and antifermion).

Next, we turn to $\Pi^{\mu\nu>}(P)D_{\nu\mu}^<(P) - \Pi^{\mu\nu<}(P)D_{\nu\mu}^>(P)$. We focus on the term $\Pi^{\mu\nu>}(P)D_{\nu\rho}^<(P)$. Similar to the fermionic case, we look at two-loop photon self-energy diagrams containing propagator corrections. There is only one such diagram shown in Fig. 2. It gives the following contribution:

$$\Pi^{\mu\nu>}(P)D_{\nu\mu}^<(P) = -e^4 \int_{K,K'} \mathrm{tr}[\gamma^\nu S^<(K)\gamma^\mu S^{22}(K+P) \times \gamma^\rho S^>(P')S^{11}(K+P)] \times D_{\rho\sigma}^>(K')D_{\nu\mu}^<(P), \qquad (45)$$

and a counterpart from $> \leftrightarrow <$ and $1 \leftrightarrow 2$ of the above. We show in Appendix A that (45) give rise to squares of s-channel Compton scattering, u-channel Compton scattering, and t-channel annihilation.

To compare with the spin-averaged Boltzmann equations by AMY [61–63], we note that square of u-channel annihilation and u-channel Coulomb (between fermions) are not present in our analysis. In fact, upon integration over phase space, they give identical contributions as their t-channel counterparts. The extra contributions in

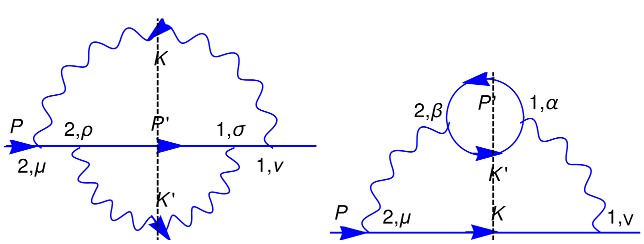

FIG. 1. Two-loop diagrams for fermion self-energy containing propagator corrections. The 12 labels are uniquely determined by the requirement that three propagators attached to a vertex cannot be simultaneously on shell. The on shell particles are indicated by a cut (dashed line) through the corresponding propagators.

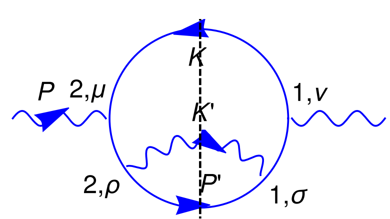

FIG. 2. Two-loop diagrams for photon self-energy containing propagator corrections. The 12 labels are uniquely determined by the requirement that three propagators attached to a vertex cannot be simultaneously on shell. The on-shell particles are indicated by a cut (dashed line) through the corresponding propagators.

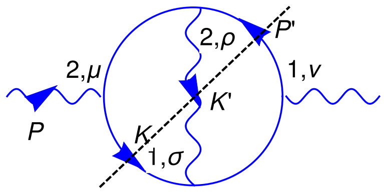

FIG. 3. Two-loop diagrams for photon self-energy containing vertex corrections. The on-shell particles are indicated by a cut (dashed line) through the corresponding propagators.

Boltzmann equations are precisely taken care of by the symmetry factor $\frac{1}{2}$ for identical particles in final states applicable for annihilation and Coulomb between fermions. Therefore, we find agreement on the square of amplitudes in all channels for the collision term.

B. Vertex corrections

The propagator corrections give square of amplitudes only. The interference between amplitudes arises from vertex corrections, which we discuss in the following. We begin with the simpler case of vertex correction in photon self-energy. In this case, only one diagram contributes, shown in Fig. 3. Its contribution to the collision term can be written as

$$\Pi^{\mu\nu>}(P)D^{<}_{\nu\mu}(P) = -e^4\int_{K,K'}\mathrm{tr}[\gamma^\mu S^>(K)\gamma^\sigma S_{11}(K+K')\times\gamma^\nu S^<(P')\gamma^\rho S_{22}(K-P)]\times D^>_{\rho\sigma}(K')D^<_{\nu\mu}(P), \tag{46}$$

and $\Pi^{\mu\nu<}(P)D^>_{\nu\mu}(P)$ obtainable from the above by $>\leftrightarrow<$ and $1\leftrightarrow 2$. In Appendix A, we show this give rise to *half* of the interference terms of s/u channels of Compton scattering and interference terms of t/u channels of annihilation.

Now, we move to the vertex correction in fermion self-energy. We have two labelings for the vertex correction diagram shown in Fig. 4. For the labeling on the left, we have the following contribution to the collision term:

$$\Sigma^>(P)S^<(P) = \int_{K,K'}\gamma^\mu S_{22}(P-K)\gamma^\nu S^>(-P')\gamma^\rho S_{11}(P-K')\times\gamma^\sigma D^>_{\nu\sigma}(K')D^>_{\mu\rho}(K)S^<(P). \tag{47}$$

We show in Appendix A that it gives rise to the following interference terms: *half* of the t/u channels for annihilation and s/t channels for Compton scattering.

For the other labeling on the right of Fig. 4, we have the following contribution to collision term:

$$\Sigma^>(P)S^<(P) = \int_{K,K'}\gamma^\mu S^>(P-K)\gamma^\nu S^<(-P')\gamma^\rho S^>(P-K')\times\gamma^\sigma D^{22}_{\mu\rho}(K)D^{11}_{\nu\sigma}(K')S^<(P). \tag{48}$$

It leads to the following interference terms: *half* of t/u channels for Coulomb scattering (between fermions) and s/t channels for Coulomb scattering (between fermion and antifermion).

Note that we have only half of the interference terms for annihilation and Coulomb scattering (between fermions). In fact, in these cases, the two interference terms are both real. Therefore, they again agree with the counterpart in the Boltzmann equation when the symmetry factor $\frac{1}{2}$ for annihilation and Coulomb scattering (between fermions) is taken into account.

To sum up, we write the elastic contribution to the loss terms on the rhs of (32) and (33) as

$$\begin{aligned}\mathrm{tr}[\Sigma^{>(0)}(P)S^{<(0)}(P)] = {}&\frac{1}{2}\int_{P',K',K'}(2\pi)^8\delta^{(4)}(P+K-P'-K')\delta(P^2-m^2)\frac{1}{16E_pE_{p'}E_kE_{k'}}\\&\times[|\mathcal{M}(P,K,P',K')|^2_{ee\to ee}f_e(P)f_e(K)(1-f_e(P'))(1-f_e(K'))\delta(K^2-m^2)\delta(P'^2-m^2)\delta(K'^2-m^2)\\&+2|\mathcal{M}(P,K,P',K')|^2_{e\bar{e}\to e\bar{e}}f_e(P)f_{\bar{e}}(K)(1-f_e(P'))(1-f_{\bar{e}}(K'))\delta(K^2-m^2)\delta(P'^2-m^2)\delta(K'^2-m^2)\\&+|\mathcal{M}(P,K,P',K')|^2_{e\bar{e}\to\gamma\gamma}f_e(P)f_{\bar{e}}(K)(1+f_\gamma(P'))(1+f_\gamma(K'))\delta(K^2-m^2)\delta(P'^2)\delta(K'^2)\\&+2|\mathcal{M}(P,K,P',K')|^2_{e\gamma\to e\gamma}f_e(P)f_\gamma(K)(1-f_e(P'))(1+f_\gamma(K'))\delta(K^2)\delta(P'^2-m^2)\delta(K'^2)],\end{aligned} \tag{49}$$

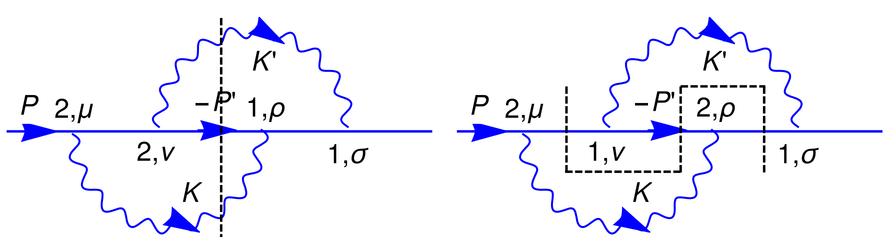

FIG. 4. Two-loop diagrams for fermion self-energy containing vertex correction. There are two possible labelings of 12. The on-shell particles are indicated by a cut (dashed line) through the corresponding propagators.

and

$$\Pi^{\mu\nu>(0)}(P)D^{<(0)}_{\nu\mu}(P) = -\frac{1}{2}\int_{P',K',K'}(2\pi)^8\delta^{(4)}(P+K-P'-K')\delta(P^2)\frac{1}{16E_pE_{p'}E_kE_{k'}} \times[|\mathcal{M}(P,K,P',K')|^2_{\gamma\gamma\to e\bar{e}}f_\gamma(P)f_\gamma(K)(1-f_e(P'))(1-f_{\bar{e}}(K'))\delta(K^2)\delta(P'^2-m^2)\delta(K'^2-m^2) + 2|\mathcal{M}(P,K,P',K')|^2_{e\gamma\to e\gamma}f_\gamma(P)f_e(K)(1+f_\gamma(P'))(1-f_e(K'))\delta(K^2-m^2)\delta(P'^2)\delta(K'^2-m^2) + 2|\mathcal{M}(P,K,P',K')|^2_{\bar{e}\gamma\to\bar{e}\gamma}f_\gamma(P)f_{\bar{e}}(K)(1+f_\gamma(P'))(1-f_{\bar{e}}(K'))\delta(K^2-m^2)\delta(P'^2)\delta(K'^2-m^2)], \quad (50)$$

respectively. By simply exchanging the initial and final states, we can obtain the corresponding gain terms, which are not shown explicitly.

C. Screening effect

The elastic collisions occur either by exchanging off-shell photons (Coulomb scattering) or by exchanging off-shell fermions (Compton scattering and annihilation). Potential IR divergences exist when the exchange particles have soft momenta. It is known that the IR divergence can be rendered finite by the screening effect. Essentially, the particles gain self-energy by interaction with the off-equilibrium medium described by kinetic theory, which effectively cuts off the divergence. The self-energy scales as $e\Lambda$ for both fermions and photons with Λ being a characteristic scale of particle energies. When $m \gg e\Lambda$, the screening effect on Compton and annihilation is negligible: the bare mass of the fermion plays the role of the cutoff. When $m \lesssim e\Lambda$, the screening effect is non-negligible. The case of Coulomb is special. Since the photon is strictly massless, the screening effect provides the only cutoff.[5] We discuss two representative scenarios: $m \gg e\Lambda$ and $m \lesssim e\Lambda$. For the former, we only need the self-energy of the photon. For the latter, we need self-energies of both the fermion and photon. All the quantities studied in this subsection are local in X; below, we suppress the dependence on X for simplicity.

Now, we work out the medium-dependent self-energy. We begin with the fermionic case. In elastic collisions, the exchanged off-shell fermion propagators S_{11}/S_{22} can be effectively replaced by S_R/S_A by using

$$S_{22}(P) = iS_A(P) + S^<(P), \\ S_{11}(P) = -iS_R(P) + S^<(P), \quad (51)$$

and the on-shell condition enforced by $S^{</>}$. Note that at the lowest order in $\hbar$, the retarded and advanced propagators are related by a "Hermitian conjugate" for fermions and a complex conjugate for photons,

$$S_A(P) = \gamma^0 S_R(P)^\dagger\gamma^0, \qquad D^A_{\mu\nu}(P) = D^{R*}_{\nu\mu}(P). \quad (52)$$

So it is sufficient to consider a medium modification to retarded propagators only. Let us consider the fermionic retarded self-energy, which satisfies the following equation:

$$i\partial\!\!\!/_x S_R(x,y) - mS_R(x,y) = -\delta(x-y) + \int d^4z\Sigma_R(x,z)S_R(z,y), \quad (53)$$

which can be derived by taking both x and y in the upper branch in (4) and subtracting the resulting equation from (7). The Wigner transform of (53) to lowest order in $\hbar$ satisfies

$$(Q\!\!\!/ - m - \Sigma_R(Q))S_R(Q) = -1, \quad (54)$$

from which we can solve for the resummed propagator,

$$S_R(Q) = -(Q\!\!\!/ - m - \Sigma_R(Q))^{-1}. \quad (55)$$

Σ_R is evaluated in Appendix B. We quote the result here,

$$\Sigma_R(Q) = e^2\int\frac{d^3p}{(2\pi)^3}\frac{1}{2p}\frac{P\!\!\!/}{P\cdot Q}(2f_\gamma(\vec{p}) + f_e(\vec{p}) + f_{\bar{e}}(\vec{p})). \quad (56)$$

Note that this result assumes $m \lesssim e\Lambda$, and we have dropped the correction to $\Sigma_R(Q)$ of order $e^3\Lambda^2/Q$ from including the fermion mass in the loop. This is justified because the correction is maximized at $Q \sim e\Lambda$, for which $Q \sim m \gg e^3\Lambda^2/Q$ so that the correction can be neglected in (54).

The photonic case is in parallel. The retarded propagator in the Coulomb gauge satisfies

$$\left(-Q^2g^{\mu\nu} + Q^\mu Q^\nu - \frac{1}{\xi}P^{\mu\alpha}P^{\nu\beta}Q_\alpha Q_\beta\right)D^R_{\nu\rho}(Q) - \Pi^{\mu\nu}_R D^R_{\nu\rho}(Q) = -\delta^\mu_\rho. \quad (57)$$

This can be solved by

[5] In fact, the screening alone is not sufficient to cut off the divergence in Coulomb. A cancellation between loss and gain terms is needed to render the corresponding collision term finite.

$$D^R_{\mu\nu}(Q) = \frac{-1}{Q^2 - \Pi^R_T} P^T_{\mu\nu} + \frac{-1}{q^2 + \Pi^R_L} u_\mu u_\nu + \xi \frac{Q_\mu Q_\nu}{q^4}, \quad (58)$$

where Π^R_T and Π^R_L are transverse and longitudinal components of the retarded photon self-energy defined as

$$\Pi^R_{\mu\nu} = P^T_{\mu\nu}\Pi^R_T - \frac{Q^2}{q^2} P^L_{\mu\nu}\Pi^R_L. \quad (59)$$

We have introduced the longitudinal projector $P^L_{\mu\nu} = -g_{\mu\nu} + \frac{Q_\mu Q_\nu}{Q^2} - P^T_{\mu\nu}$ and $q^2 = -Q^2 + (Q\cdot u)^2$. We again set $\xi = 0$ for the Coulomb gauge. $\Pi^R_{\mu\nu}$ is evaluated in Appendix B. We quote the result here,[6]

$$\Pi^R_{\mu\nu}(Q) = 2e^2 \int \frac{d^3p}{(2\pi)^3} \frac{1}{E_p} (f_e(\vec{p}) + f_{\bar{e}}(\vec{p})) \times \left[\frac{P_\mu Q_\nu + P_\nu Q_\mu - g_{\mu\nu} P\cdot Q}{P\cdot Q} - \frac{P^\mu P^\nu Q^2}{(P\cdot Q)^2}\right], \quad (60)$$

which is applicable for both scenarios with mass dependence implicit in $E_p = \sqrt{p^2 + m^2}$. We iterate that the following replacements with resummed propagators are to be used in the evaluation of self-energies when exchanged particles have soft momenta,

$$S_{22}(P) \to iS_A(P), \qquad S_{11}(P) \to -iS_R(P),$$
$$D^{\mu\nu}_{22}(P) \to iD^{\mu\nu}_A(P), \qquad D^{\mu\nu}_{11}(P) \to -iD^{\mu\nu}_R(P). \quad (61)$$

We also need the asymptotic thermal mass for hard on-shell fermions and transverse photons in inelastic collisions in the next section, which we determine below. Equation (54) determines the fermion dispersion relation by

$$\not{Q} - m - \Sigma_R(Q) = 0. \quad (62)$$

Following [72], we decompose the self-energy as $\Sigma_R = \Sigma^R_\mu \gamma^\mu + \Sigma^R_m 1$, which allows us to convert the matrix equation (62) into a scalar equation,

$$(Q_\mu - \Sigma^R_\mu)^2 - (\Sigma^R_m + m)^2 = 0. \quad (63)$$

From (56), we have $\Sigma^R_\mu \sim e^2\Lambda$ and $\Sigma^R_m = 0$. The thermal mass is identified as

$$\delta m_e^2 = 2Q^\mu \Sigma^R_\mu = e^2 \int \frac{d^3p}{(2\pi)^3} \frac{2}{p} (2f_\gamma(\vec{p}) + f_e(\vec{p}) + f_{\bar{e}}(\vec{p})). \quad (64)$$

The only change from the resummed propagator in equilibrium is that the thermal mass depends on the off-equilibrium distributions for fermions and photons.

The photon thermal mass is determined from the pole of the transverse component of the propagator as

$$m_\gamma^2 = \Pi^R_T = \frac{1}{2} P^T_{\mu\nu}\Pi^{\mu\nu}_R. \quad (65)$$

The term $P_\mu Q_\nu + P_\nu Q_\mu$ in (60) is eliminated upon contraction with $P^T_{\mu\nu}$, and the term containing Q^2 vanishes by the on-shell condition, leaving the following Q-independent expression:

$$m_\gamma^2 = e^2 \int \frac{d^3p}{(2\pi)^3} \frac{2}{E_p} (f_e(\vec{p}) + f_{\bar{e}}(\vec{p})). \quad (66)$$

Summarizing this section, by considering propagator and vertex corrections, we have captured the full $2 \to 2$ elastic collision including the screening effect in the Boltzmann equation for QED.

IV. INELASTIC COLLISIONS

In the analysis of elastic scattering, we have excluded one-loop contributions to self-energies, which require all three particles to be exactly collinear, leaving a vanishing phase space. In fact, it is not entirely excluded; when we take into account medium modification of energy of on-shell degree of freedoms, the energy conservation can be slightly violated, opening up a small phase space. It is known that in equilibrium medium both fermions and photons gain thermal mass and damping rate, which modifies the energy by an amount of order $e^2\Lambda$. Such a modification can also be realized by transverse momenta of order $e\Lambda$. It implies that medium modification to energy allows for deviation of collinearity with transverse

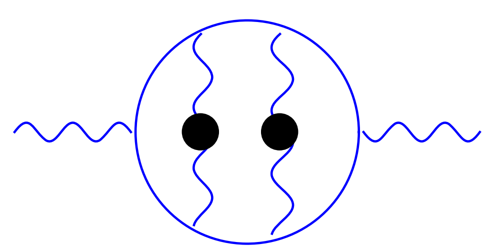

FIG. 5. Photon self-energy containing vertex corrections from multiple scatterings. An arbitrary number of soft photon exchanges is possible. For illustration purposes, we show two photon exchanges. The black dots indicate resummed photon propagators.

[6]For an anisotropic medium, for example, a medium with shear gradient, the gradient correction to $f_{e/\bar{e}}$ can give rise to additional structures not present in (59). These corrections introduce a subleading effect on screening, which is suppressed by the factor $\frac{\partial_X f}{\Lambda} \ll 1$. We can ignore such a correction in screening as long as we are concerned with leading order effect of the gradient.

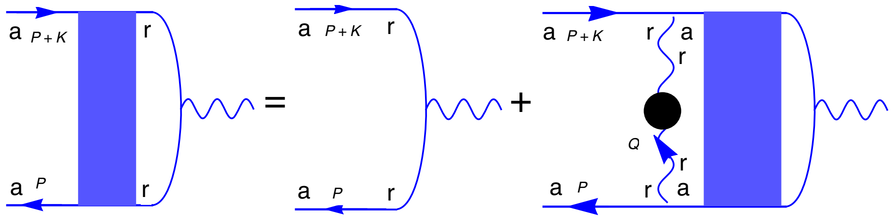

FIG. 6. Diagrammatic equation satisfied by the resummed vertex. We consider a spin-dependent vertex, where the fermions with momenta $P+K$ and P carry spin labels s and t.

momenta of order $e\Lambda$, which gives rise to a phase space $\frac{d^2p_\perp dp_\parallel}{E_p} \sim e^2\Lambda^2$. Combining this with e^2 from vertices in a one-loop diagram, we have an overall $e^4\Lambda^2$, which is the same as the two-loop diagrams. In fact, fermions can have multiple soft scatterings with the medium, which by a pinching mechanism all contribute at the same order and need to be added coherently, known as the Landau-Pomeranchuk-Migdal effect. The multiple scatterings are encoded in another type of vertex corrections in self-energies diagrams, shown in Fig. 5. It involves multiple insertions of soft photon propagators. When there is no insertion of a photon propagator, it reduces to a one-loop diagram, for which the power counting is done above. Below, we confirm that the power counting is not affected by insertions of photon propagators.

A. Resummed vertex

Let us illustrate the pinching mechanism by looking at the resummed vertex. Following [73], the evaluation is most conveniently done in the ra basis, in which only one inequivalent labeling is allowed.[7] The resummed vertex satisfies the diagrammatic equation in Fig. 6. The pinching mechanism can be seen by inspecting the energy integration of two side rails,

$$\int \frac{dp_0}{2\pi} S_{ra}(P)(\cdots)S_{ar}(K+P), \tag{67}$$

with $S_{ra} = D_{ra}(P)(\not{P}+m)$ and $S_{ar} = D_{ar}(K+P)\times(\not{K}+\not{P}+m)$. D_{ra} and D_{ar} are the same as scalar propagators given by[8]

$$D_{ra}(P) = \frac{i}{(p_0+\frac{i}{2}\Gamma_p)^2 - E_p^2},$$
$$D_{ar}(K+P) = \frac{i}{(p_0+k_0-\frac{i}{2}\Gamma_{p+k})^2 - E_{p+k}^2}. \tag{68}$$

To be specific, we take $k_0 > 0$. Let us evaluate the following by residue theorem,

$$\int \frac{dp_0}{2\pi} D_{ra}(P)D_{ar}(K+P). \tag{69}$$

The poles are located at $p_0 = \pm E_p - \frac{i}{2}\Gamma_p$, $p_0 = -k_0 \pm E_{p+k} + \frac{i}{2}\Gamma_{p+k}$. Here, P is allowed to have transverse component $p_\perp \sim e\Lambda$. Here, the energies of both fermions and photons receive corrections from deviation of collinearity and thermal/bare mass. Note that the photon momentum is used to define longitudinal direction, so it has no deviation from collinearity,

$$E_p = p + \frac{p_\perp^2 + \delta m_e^2 + m^2}{2p},$$
$$E_{p+k} = |\mathbf{p}+\mathbf{k}| + \frac{p_\perp^2 + \delta m_e^2 + m^2}{2|\mathbf{p}+\mathbf{k}|},$$
$$k_0 = k + \frac{m_\gamma^2}{2k}. \tag{70}$$

Denoting $p_\parallel = \vec{p}\cdot\hat{k}$, we can rewrite the poles as $p_0 = \pm p_\parallel - \frac{i}{2}\Gamma_p$, $p_0 = -k_0 \pm (p_\parallel + k) + \frac{i}{2}\Gamma_{p+k}$. The pinching mechanism is at work when two of the poles nearly pinch. Ignoring the thermal masses and damping rate, we find the poles at $p_0 = p_\parallel$ and $p_0 = -k_0 + p_\parallel + k$ coincide. The thermal masses and damping rates provide necessary regularization to the divergence. Closing the contour and picking up one of the pinching poles, we obtain

$$\int \frac{dp_0}{2\pi} D_{ra}(P)D_{ar}(K+P) = \frac{-1}{4p_\parallel(p_\parallel+k)(i\delta E+\Gamma)}, \tag{71}$$

with

$$\delta E = k_0 + E_p\epsilon(p_\parallel) - E_{p+k}\epsilon(p_\parallel + k)$$
$$\simeq \frac{k(p_\perp^2 + \delta m_e^2 + m^2)}{2p_\parallel(p_\parallel+k)} + \frac{m_\gamma^2}{2k},$$
$$\Gamma = \frac{1}{2}(\Gamma_p + \Gamma_{p+k}). \tag{72}$$

In addition, each pair of pinching propagators (side rails) is accompanied by a soft photon propagator (rung). The power counting for the latter is done as follows: note that the momentum Q of the off-shell photon is space-like, and

[7] The other one is related by interchanging r and a. All other labelings can be related to the two.
[8] $\frac{\Gamma}{2}$ is defined as the damping rate here.

its time component fixed the pinching conditions as $\int dq_0\delta(p_0-p_\parallel)\delta(p_0-q_0-p_\parallel-q_\parallel)=\delta(p_0-p_\parallel)$, so that the phase space for Q counts as e^3. The power counting for the relevant propagator $D_{rr}(Q)$ can be done using its equilibrium form $D_{rr}(Q)=(\frac{1}{2}+f(q_0))\rho(Q)$. Using the spectral density $\rho(Q)\sim Q^{-2}\sim e^{-2}$ and the Bose enhancement factor $f(q_0)\sim q_0^{-1}\sim e^{-1}$, we have $D_{rr}(Q)\sim e^{-3}$. Combining pieces together with an e^2 from extra vertices, we obtain for each one pair of side rails and one rung,

$$\frac{1}{i\delta E+\Gamma}e^3e^{-3}e^2\sim\frac{e^2}{i\delta E+\Gamma}. \tag{73}$$

In the scenario $m\lesssim e\Lambda$, $\delta E\sim e^2\Lambda$ and Γ are evaluated in Appendix C to be at the same order. Thus, we have from (73) an overall factor e^0; thus, the arbitrary number of insertions are allowed, corresponding to multiple soft scatterings of hard fermions with the medium fermions. However, in the scenario $m\gg e\Lambda$, the pinching mechanism is suppressed by a factor of $\frac{e^2\Lambda^2}{m^2}$. It follows that inelastic scattering is irrelevant in this scenario to the order of our interest. Below, we proceed with the scenario $m\lesssim e\Lambda$.

We denote the resummed vertex in Fig. 6 as $\Gamma^\mu_{st}(P+K,P)$, with s, t labeling the spinors in the outermost propagators carrying momenta $P+K$ and P, respectively. This is a polarization-dependent vertex between two on-shell fermions with spin s, t and one on-shell photon. We can take the Lorentz index μ to be transverse, since the resulting self-energy will be contracted with a projector in (33). Below, we denote μ by M for transverse indices. Below, we first consider the case $p_0>0$, for which Γ^M_{st} can be interpreted as the amplitude of a fermion (with momentum $P+K$ and spin s) splitting into a fermion (with momentum P and spin t) and a photon (with momentum K and polarization ϵ^M). We can express the diagrammatic equation as[9]

$$\begin{aligned}\Gamma^M_{st}&(P+K,P)\\ &=D_{ra}(P)D_{ar}(P+K)u_s(P+K)\bar u_s(P+K)\gamma^M u_t(P)\bar u_t(P)\\ &\quad+\int_Q D_{ra}(P)D_{ar}(P+K)((\not P+\not K)(-ie\gamma^\mu)\\ &\quad\times\Gamma^M_{st}(P+K+Q,P+Q)(-ie\gamma^\nu)\not P)D^{rr}_{\nu\mu}(Q),\end{aligned} \tag{74}$$

where the structures $u_s(P+K)\bar u_s(P+K)$ and $u_t(P)\bar u_t(P)$ come from $\not P+\not K$ and $\not P$ projected onto given spin states, respectively. Note that we have dropped the subleading masses in the numerators of fermion propagators. We use the following representation for spinors:

$$u_s(P)=\sqrt{\frac{p_0}{2}}\begin{pmatrix}(1-\sigma\cdot\vec p/p_0)\xi_s\\(1+\sigma\cdot\vec p/p_0)\xi_s\end{pmatrix}, \tag{75}$$

with $\xi_+=(1,0)^T$ and $\xi_-=(0,1)^T$. In this representation, the spin label $s=\pm$ corresponds to spin being parallel/antiparallel to momentum. We can derive the following relations as valid to leading order in e:

$$\begin{aligned}&\bar u_s(P+K)\gamma^\mu u_{s'}(P+Q+K)\simeq\delta_{ss'}2(P+K)^\mu,\\ &\qquad\bar u_{t'}(P+Q)\gamma^\nu u_t(P)\simeq\delta_{tt'}2P^\nu,\\ &\qquad\bar u_s(P+K)\gamma^M u_t(P)\simeq(p_\parallel(p_\parallel+k))^{-1/2}\\ &\qquad\qquad\times((p_\parallel+k)p_\parallel^M+p_\parallel p^M_{-s})\delta_{st},\end{aligned} \tag{76}$$

with $p^M_\pm=p^M\pm i\epsilon^{MN}p^N$, and we have used the pinching condition $p_0\simeq p_\parallel$. We easily deduce that the spin direction of the fermion along the upper/lower rails is not changed. We can parametrize the vertex by

$$\begin{aligned}\Gamma^M_{st}(P+K,P)&=\delta_{st}u_s(P+K)\bar u_t(P)(p_\parallel(p_\parallel+k))^{-1/2}\\ &\quad\times((p_\parallel+k)p^M_s+p_\parallel p^M_{-s})\Gamma_s(P).\end{aligned} \tag{77}$$

By rotational invariance, $\Gamma(P)$ is a function of $p_\parallel$, $p_\perp^2$. It follows then that

$$\begin{aligned}&((p_\parallel+k)p^M_s+p_\parallel p^M_{-s})\Gamma_s(P)\\ &\quad=((p_\parallel+k)p^M_s+p_\parallel p^M_{-s})D_{ra}(P)D_{ar}(P+K)\\ &\qquad-e^2\int_Q D_{ra}(P)D_{ar}(P+K)((p_\parallel+k)(p+q)^M_s\\ &\qquad+p_\parallel(p+q)^M_{-s})\Gamma_s(P+Q)4p_\parallel(p_\parallel+k)\\ &\qquad\times\hat K^\mu\hat K^\nu D^{rr}_{\nu\mu}(Q).\end{aligned} \tag{78}$$

By the pinching mechanism, the vertex should have support localized on the pole $p_0=p_\parallel$. The same kinematic restriction should apply to the bare vertex in the diagrammatic equation in Fig. 6. It is then convenient to define

$$\int\frac{dp_0}{2\pi}\Gamma_s(P)=-\frac{1}{4p_\parallel(p_\parallel+k)}\chi_s(P). \tag{79}$$

In terms of χ_s, (78) becomes

$$\begin{aligned}&-((p_\parallel+k)p^M_s+p_\parallel p^M_{-s})\chi_s(P)(i\delta E+\Gamma)\\ &\quad=-((p_\parallel+k)p^M_s+p_\parallel p^M_{-s})\\ &\qquad-e^2\int\frac{d^3q}{(2\pi)^3}((p_\parallel+k)(p+q)^M_s\\ &\qquad+p_\parallel(p+q)^M_{-s})\chi_s(P+Q)\hat K^\mu\hat K^\nu D^{rr}_{\nu\mu}(Q).\end{aligned} \tag{80}$$

Equation (80) can be further simplified by using the following representation of Γ:

[9] An overall $-ie$ is factored out from the vertex.

$$\Gamma = e^2 \int \frac{d^3q}{(2\pi)^3} \hat{K}^\mu \hat{K}^\nu D^{rr}_{\nu\mu}(Q). \quad (81)$$

It contains the same soft photon propagator as in (80). A derivation of the representation can be found in Appendix C. Using (81), we can rewrite (80) as

$$\begin{aligned}
&((p_\parallel + k)p^M_s + p_\parallel p^M_{-s}) \\
&= ((p_\parallel + k)p^M_s + p_\parallel p^M_{-s})\chi_s(P)i\delta E \\
&\quad + e^2 \int \frac{d^3q}{(2\pi)^3} \hat{K}^\mu \hat{K}^\nu D^{rr}_{\nu\mu}(Q) \\
&\quad \times [((p_\parallel + k)p^M_s + p_\parallel p^M_{-s})\chi_s(P+Q) \\
&\quad - ((p_\parallel + k)(p+q)^M_s + p_\parallel (p+q)^M_{-s})\chi_s(P+Q)]. \quad (82)
\end{aligned}$$

The structure $(p_\parallel + k)p^M_s + p_\parallel p^M_{-s}$ encodes the spin dependence of the vertex. It is more transparent to switch to circular polarizations for the photon $\epsilon^M_\pm = \frac{1}{\sqrt{2}}(0, 1, \pm i, 0)$. The corresponding coordinates and momenta are defined by $x^\pm = \frac{1}{\sqrt{2}}(x \pm iy)$ and $p^\pm = \frac{1}{\sqrt{2}}(p_x \pm i p_y)$, with $M = \pm$ in the circular basis. Using $p^M_+ = (\sqrt{2}p^+, 0)$, $p^M_- = (0, \sqrt{2}p^-)$, we find (82) splits into two cases $s = \pm M$, which satisfy a unified equation

$$\begin{aligned}
p^M = p^M\chi_s(P)i\delta E + e^2 \int \frac{d^3q}{(2\pi)^3} \hat{K}^\mu \hat{K}^\nu D^{rr}_{\nu\mu}(Q) \\
\times [p^M\chi_s(P+Q) - (p+q)^M\chi_s(P+Q)]. \quad (83)
\end{aligned}$$

Recall in our $\hbar$ expansion that f_e is spin independent. It follows from (B13) and (B15) that the kernel $\hat{K}^\mu \hat{K}^\nu D^{rr}_{\nu\mu}(Q)$ is also spin independent. A spin-independent $\chi_s = \chi$ is expected from (83). Furthermore, (83) is manifestly rotational invariant, which is equally valid in the orthogonal basis. Equation (83) in the orthogonal basis is in agreement with Eqs. (2.2) and (2.6) of [61], with the identification $\chi = \frac{1}{2}\chi_{AMY}$.

Although spin information is averaged out in the resulting kinetic theory, the spin dependence of the vertex is instructive on its own. The structure $(p_\parallel + k)p^M_s + p_\parallel p^M_{-s}$ in a circular basis indicates that a fermion with spin in either direction can radiate a right-/left- handed photon without changing its spin. Clearly spin angular momentum is not conserved. Since collision is local, orbital angular momentum is zero before and after the collision. The change of the spin angular momentum comes from spin exchange between the fermion/photon in the resummed vertex and fermions in the medium, whose spin information is averaged out.

B. Photon self-energy

From Fig. 6, the resummed vertex Γ^M_{st} contains the four fermi correlators $G_{\rm aarr}(P+K, P, P+K+Q, P+Q)$ with $P+K$ and P labeled by a and $P+K+Q$ and $P+Q$ labeled by r as in Fig. 6. In the pinching kinematical region, $Q \ll P\,\&\,K$. To convert to photon self-energy, we need $G_{1122}(P+K, P, P+K+Q, P+Q)$. The conversion involves an off-equilibrium generalization of the Kubo-Martin-Schwinger (KMS) relation. We give a diagrammatic derivation of the relation in the pinching kinematical region in Appendix D. The off-equilibrium relation simply replaces the equilibrium distribution by the off-equilibrium counterpart as

$$\begin{aligned}
&G_{1122}(P+K, P, P+K+Q, P+Q) \\
&\quad = f_e(p_\parallel + k)(1 - f_e(p_\parallel)) \\
&\qquad \times 2{\rm Re}G_{\rm aarr}(P+K, P, P+K+Q, P+Q). \quad (84)
\end{aligned}$$

Accordingly, to obtain the photon self-energy $\Pi^<(K) = \int_{P,Q} G_{1122}(P+K, P, P+K+Q, P+Q)$, we should use $f_e(p_\parallel + k)(1 - f_e(p_\parallel))2{\rm Re}[\Gamma^M_{st}]$ as the correct resummed vertex. Now, we can trace $-ie\Gamma^M_{st}(P+K, P)$ with $-ie\gamma^N$, include -1 from the fermion loop, sum over spins, and integrate over momentum to obtain

$$\begin{aligned}
\Pi^{<MN}(K) &= \int_P (-1)(-ie)^2 \sum_{s,t} {\rm tr}[\Gamma^M_{st}(P+K, P)\gamma^N] \\
&= e^2 \sum_s \int \frac{d^3p}{(2\pi)^3} \frac{1}{4(p_\parallel(p_\parallel + k))^{3/2}} \\
&\quad \times ((p_\parallel + k)p^M_s + p_\parallel p^M_{-s}) f_e(p_\parallel + k)(1 - f_e(p_\parallel)) \\
&\quad \times 2{\rm Re}[\chi(P)]{\rm tr}[u_s(P+K)\bar{u}_s(P)\gamma^N]. \quad (85)
\end{aligned}$$

Recall in (33), $\Pi^{<MN}$ is contracted with $D^>_{MN}(K) \propto P^T_{MN} f_\gamma(k)$. We can use the following for the trace:

$$\begin{aligned}
&{\rm tr}[u_s(P+K)\bar{u}_s(P)\gamma^N] \\
&\quad = (p_\parallel(p_\parallel + k))^{-1/2}((p_\parallel + k)p^N_{-s} + p_\parallel p^N_s). \quad (86)
\end{aligned}$$

By the s-independent identity,

$$\sum_M p^M_s p^M_{-s} = 2p^2_\perp, \qquad \sum_M p^M_s p^M_s + p^M_{-s} p^M_{-s} = 0, \quad (87)$$

we can see that the spin sum simply gives a factor of 2. In the end, we arrive at

$$\begin{aligned}
\Pi^{<MN} D^>_{MN} = e^2 \int \frac{d^3p}{(2\pi)^3} f_e(p_\parallel + k)(1 - f_e(p_\parallel))(1 + f_\gamma(k)) \\
\times 2{\rm Re}[\chi(P)] \frac{((p_\parallel + k)^2 + p^2_\parallel)p^2_\perp}{(p_\parallel(p_\parallel + k))^2}. \quad (88)
\end{aligned}$$

The other collision term $\Pi^{>MN} D^<_{MN}$ is obtainable from (88) by the replacement of the distribution functions $f_e(p_\parallel + k)(1 - f_e(p_\parallel))(1 + f_\gamma(k)) \to (1 - f_e(p_\parallel + k)) f_e(p_\parallel) f_\gamma(k)$.

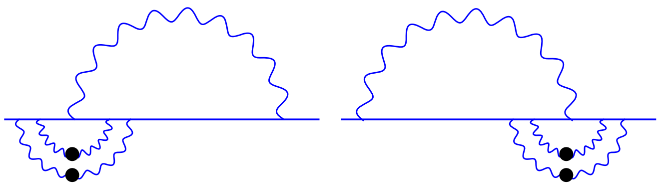

FIG. 7. Fermion self-energy containing vertex corrections from multiple scatterings. An arbitrary number of soft photon exchanges is possible. Unlike the photonic case, there are two inequivalent vertex corrections.

So far, we have focused on the kinematical region with $p_0 > 0$ and $k_0 > 0$. Let us first lift $p_0 > 0$. Other possible kinematical regions are $p_0 + k < 0$ corresponding to antifermion bremsstrahlung and $-k < p_0 < 0$ corresponding to inelastic annihilation. For $p_0 + k < 0$, we use the following projections for spin states:

$$\begin{aligned} \not{P} + \not{K} &\to -u_s(-P-K)\bar{u}_s(-P-K), \\ \not{P} &\to -u_t(-P)\bar{u}_t(-P). \end{aligned} \tag{89}$$

The contraction of vertices is modified slightly from (76) as

$$\begin{aligned} \bar{u}_s(-P-K)\gamma^\mu u_{s'}(-P-Q-K) &\simeq -\delta_{ss'} 2(P+K)^\mu, \\ \bar{u}_{t'}(-P)\gamma^\nu u_t(-P-Q) &\simeq -\delta_{tt'} 2P^\nu, \\ \bar{u}_s(-P-K)\gamma^M u_t(-P) &\simeq (p_\parallel (p_\parallel + k))^{-1/2} \\ &\quad \times ((p_\parallel + k)p_\parallel^M + p_\parallel p_{-s}^M)\delta_{st}. \end{aligned} \tag{90}$$

With these, we easily confirm that (88) is also applicable for $p_0 < -k$. The analysis for $-k < p_0 < 0$ is similar, with $p_\parallel(p_\parallel + k)$ replaced by $-p_\parallel(p_\parallel + k)$, which leaves (88) unchanged. This justifies extending the integration domain of $p_\parallel$ to $(-\infty, \infty)$.

Finally, we comment on the case $k_0 < 0$. This case would be needed for the dynamics of photon's antiparticle. Since the photon's antiparticle is itself, we expect it to give an equivalent equation.

C. Fermion self-energy

Unlike the photonic case, the fermion self-energy arises from two diagrams shown in Fig. 7. To be specific, let us consider $p_0 > 0$ corresponding to a fermion. We consider the term $\Sigma^> S^< (\Sigma^< S^>)$ and focus on the second diagram first. It is convenient to include the contribution $\Sigma_{22} S_{22} (\Sigma_{11} S_{11})$. Upon taking the trace, we have from the diagrammatic identity in Fig. 8 that

$$\begin{aligned} &\mathrm{tr}[\Sigma^>(P)S^<(P) + \Sigma_{22}(P)S_{22}(P)] \\ &\quad = \int_K [G^{\mu\nu>}(P+K,P)D^<_{\nu\mu}(K) + G^{\mu\nu}_{22}(P+K,P)D^{22}_{\nu\mu}(K)], \\ &\mathrm{tr}[\Sigma^<(P)S^>(P) + \Sigma_{11}(P)S_{11}(P)] \\ &\quad = \int_K [G^{\mu\nu<}(P+K,P)D^<_{\nu\mu}(K) + G^{\mu\nu}_{11}(P+K,P)D^{11}_{\nu\mu}(K)], \end{aligned} \tag{91}$$

where $G^{\mu\nu}(P+K,P)$ are partially integrated photon self-energies defined as

$$\begin{aligned} G^{\mu\nu>}(P+K,P) &= \int_Q \mathrm{tr}[(-ie\gamma^\mu)G_{2211}(P+K,P,P+K+Q,P+Q)(-ie\gamma^\nu)], \\ G^{\mu\nu<}(P+K,P) &= \int_Q \mathrm{tr}[(-ie\gamma^\mu)G_{1122}(P+K,P,P+K+Q,P+Q)(-ie\gamma^\nu)], \\ G^{\mu\nu}_{22}(P+K,P) &= \int_Q \mathrm{tr}[(-ie\gamma^\mu)G_{2222}(P+K,P,P+K+Q,P+Q)(-ie\gamma^\nu)], \\ G^{\mu\nu}_{11}(P+K,P) &= \int_Q \mathrm{tr}[(-ie\gamma^\mu)G_{1111}(P+K,P,P+K+Q,P+Q)(-ie\gamma^\nu)]. \end{aligned}$$

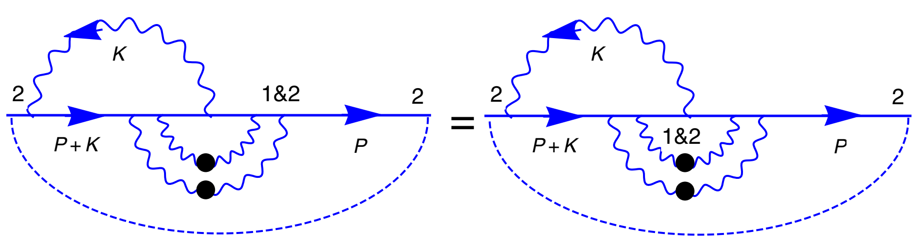

FIG. 8. The lhs and rhs have one-to-one correspondence with the first line of (91). The symbol 1&2 indicates the vertex can be labeled by either 1 or 2, giving rise to two terms. The dashed line corresponds to the trace in the left diagram and the contraction in the right diagram. Replacing the outermost labels 2 by 1 leads to the second line of (91).

Taking the difference of the two lines in (91), we obtain (with arguments suppressed)

$$\mathrm{tr}[\Sigma^{>}S^{<}-\Sigma^{<}S^{>}+\Sigma_{22}S_{22}-\Sigma_{11}S_{11}] = \int_K [G^{\mu\nu>}D^{>}_{\nu\mu}-G^{\mu\nu<}D^{<}_{\nu\mu}+G^{\mu\nu}_{22}D^{22}_{\nu\mu}-G^{\mu\nu}_{11}D^{11}_{\nu\mu}]. \quad (92)$$

Using that $\Sigma^{>/<}$ and $S^{>/<}$ are "Hermitian", we can easily show that $\mathrm{tr}[\Sigma^{>}S^{<}-\Sigma^{<}S^{>}]$ is real. Further using the following Hermitian properties,

$$\Sigma_{22}=\gamma^0\Sigma_{11}^{\dagger}\gamma^0, \qquad S_{22}=\gamma^0 S_{11}^{\dagger}\gamma^0,$$
$$G^{\mu\nu}_{22}=G^{\nu\mu *}_{11}, \qquad D^{\mu\nu}_{22}=D^{\nu\mu *}_{11}, \quad (93)$$

we obtain from (92)

$$\begin{aligned}\mathrm{tr}[\Sigma^{>}(P)S^{<}(P)-\Sigma^{<}(P)S^{>}(P)] &= \mathrm{Re}(\mathrm{tr}[\Sigma^{>}(P)S^{<}(P)-\Sigma^{<}(P)S^{>}(P)]) \\ &= \int_K [G^{\mu\nu>}(P+K,P)D^{<}_{\nu\mu}(K)-G^{\mu\nu<}(P+K,P)D^{>}_{\nu\mu}(K)]. \end{aligned} \quad (94)$$

The evaluation of the first diagram proceeds similarly. We have instead

$$\mathrm{tr}[\Sigma^{>}(P)S^{<}(P)-\Sigma^{<}(P)S^{>}(P)] = \int_K [G^{\mu\nu<}(P,P+K)D^{<}_{\nu\mu}(K)-G^{\mu\nu>}(P,P+K)D^{>}_{\nu\mu}(K)]. \quad (95)$$

Note that the momenta arguments in (94) and (95) differ. Using $G^{\mu\nu<}(P,P+K)=G^{\nu\mu>}(P+K,P)$ and the fact that $D^{</>}_{\nu\mu}$ is symmetric in $\mu\nu$, we easily see that the two diagrams give identical contributions. One may wonder about the contribution when both vertices are resummed. We show by enumeration in Appendix E that such a contribution is not allowed.

Note that $p_0=p$ with our choice. It is useful to rearrange our results above. Using the reciprocal relations (21) and (31), we can deduce that a diagrammatically analogous relation holds for fermion self-energy from the pinching kinematical region,

$$\Sigma^{>}(P)=\bar{\Sigma}^{<}(-P)=\Sigma^{<}(-P). \quad (96)$$

In the second equality, we have removed the overline because we have dropped the subleading mass next to $\not{P}$, and the mass always appears in squares elsewhere. We can then rewrite

$$\mathrm{tr}[\Sigma^{>}(P)S^{<}(P)]|_{\mathrm{2nd}}=\mathrm{tr}[\Sigma^{<}(-P)S^{>}(-P)]|_{\mathrm{1st}},$$
$$\mathrm{tr}[\Sigma^{<}(P)S^{>}(P)]|_{\mathrm{2nd}}=\mathrm{tr}[\Sigma^{>}(-P)S^{<}(-P)]|_{\mathrm{1st}}, \quad (97)$$

where the subscripts 1st and 2nd denote contributions from the first and second diagrams in Fig. 7, respectively. This allows us to reexpress the contributions in the region $p_0=p$ from two diagrams to the counterpart in the region $p_0=\pm p$ from a single diagram,

$$\begin{aligned}\mathrm{tr}[\Sigma^{>}(P)S^{<}(P)-\Sigma^{<}(P)S^{>}(P)]_{\mathrm{1st+2nd}} &= \mathrm{tr}[\Sigma^{>}(P)S^{<}(P)-\Sigma^{<}(P)S^{>}(P)-\Sigma^{>}(-P)S^{<}(-P) \\ &\quad +\Sigma^{<}(-P)S^{>}(-P)]_{\mathrm{1st}}. \end{aligned} \quad (98)$$

In fact, the rhs of (98) is closely related to (88). Note that $\Pi^{MN</>}(K)=\int_P G^{MN</>}(P+K,P)$. We would have the collision term of the photon if the momentum integration is done over P instead of K. To establish the relation, we first integrate $G^{MN</>}$ over transverse components of momentum so that the resulting collision term has a natural interpretation as collinear $1\leftrightarrow 2$ processes. This can be conveniently done by converting $d^2k_\perp$ to $d^2p_\perp$. The key observation is that the geometrically invariant quantity here is the opening angle θ between $\vec{p}$ and $\vec{k}$, which is bounded by the integrand as $\theta\lesssim\frac{m_\gamma}{p}\sim O(e)$. Using spherical coordinates, we can easily show

$$\int\frac{d^2k_\perp}{(2\pi)^2}=\frac{k^2}{p^2}\int\frac{d^2p_\perp}{(2\pi)^2}. \quad (99)$$

The remaining complication is in the integration of k_0. On one hand, $G^{MN</>}$ contains $\delta(p_0-p_\parallel\epsilon(k_0))$ according to the pinching mechanism. On the other hand, $\delta(K^2)$ from $D^{</>}_{MN}=\frac{1}{2k}(\delta(k_0-k)+\delta(k_0+k))$ receives contributions from two poles. For $k_0=k$, it gives the following contribution:

$$\begin{aligned}\int_K G^{MN>}D^{<}_{MN} &= \int_0^\infty\frac{dk}{2\pi}\int\frac{d^2p_\perp}{(2\pi)^2}\frac{k}{2p^2}f_e(p_\parallel)(1-f_e(p_\parallel+k)) \\ &\quad\times 2\mathrm{Re}[\chi(P)]2\pi\delta(p_0-p_\parallel) \\ &\quad\times\frac{((p_\parallel+k)^2+p_\parallel^2)p_\perp^2}{(p_\parallel(p_\parallel+k))^2}2\pi(1+f_\gamma(K)). \end{aligned} \quad (100)$$

For $k_0<-k$, we have instead

$$\begin{aligned}\int_K G^{MN>}D^{<}_{MN} &= \int_0^\infty\frac{dk}{2\pi}\int\frac{d^2p_\perp}{(2\pi)^2}\frac{k}{2p^2} \\ &\quad\times f_e(-p_\parallel)(1-f_e(-p_\parallel-k)) \\ &\quad\times 2\mathrm{Re}[\chi(P)]2\pi\delta(p_0+p_\parallel) \\ &\quad\times\frac{((-p_\parallel-k)^2+p_\parallel^2)p_\perp^2}{(-p_\parallel(-p_\parallel-k))^2}2\pi(1+f_\gamma(K)). \end{aligned} \quad (101)$$

Note that we need to have $p_\parallel>0(p_\parallel<0)$ for $k_0>0(k_0<0)$, respectively, in order to give the pole contribution at $p_0 = p$ for fermion. We can then combine (100) and (101) to write

$$\begin{aligned}
&\mathrm{tr}[\Sigma^>(P)S^<(P) - \Sigma^<(P)S^>(P)] \\
&\quad = \int \frac{dk_\parallel}{2\pi} \int \frac{d^2 p_\perp}{(2\pi)^2} \frac{k}{2p^2} f_e(p)(1 - f_e(p + k_\parallel)) \\
&\qquad \times 2\mathrm{Re}[\chi(P)] 2\pi\delta(p_0 - p) \frac{((p + k_\parallel)^2 + p^2)p_\perp^2}{(p(p + k_\parallel))^2} \\
&\qquad \times 2\pi(1 + f_\gamma(K)). \qquad (102)
\end{aligned}$$

Equation (102) is in agreement with Eq. (5.3) of [61] when specialized to the $U(1)$ gauge group.

V. QUANTUM CORRECTION

Now, we proceed to the quantum correction, which captures dynamics of spin polarization. We first consider the quantum correction to the fermion Wigner function $S^{<(1)}$, which enters two equations from the expansion in $\hbar$ at different orders,

$$\begin{aligned}
\frac{i}{2}\partial\!\!\!/ S^{<(0)} + \frac{P\!\!\!/ - m}{\hbar} S^{<(1)} &= \frac{i}{2}(\Sigma^{>(0)}S^{<(0)} - \Sigma^{<(0)}S^{>(0)}), \\
\frac{i}{2}\partial\!\!\!/ S^{<(1)} + \frac{P\!\!\!/ - m}{\hbar} S^{<(2)} &= \frac{i}{2}(\Sigma^{>(1)}S^{<(0)} - \Sigma^{<(1)}S^{>(0)} \\
&\quad + \Sigma^{>(0)}S^{<(1)} - \Sigma^{<(0)}S^{>(1)}) \\
&\quad - \frac{\hbar}{4}(\{\Sigma^{>(0)}, S^{<(0)}\}_{\mathrm{PB}} \\
&\quad - \{\Sigma^{<(0)}, S^{>(0)}\}_{\mathrm{PB}}). \qquad (103)
\end{aligned}$$

Recall that the trace of the first equation has been used to derive the classical kinetic equation. The off-diagonal components serve as a constraint equation for $S^{<(1)}$. It determines the nondynamical part of $S^{<(1)}$. The second equation is dynamical for $S^{<(1)}$. Its role is similar to that of the first equation to $S^{<(0)}$. We expect that the second equation would give rise to an additional axial component of $S^{<(1)}$ in the form $a^\mu f_A$ with $f_A \sim O(\frac{\hbar\partial_X f}{\Lambda})$. Note that although f_A is excluded by the parity invariant assumption at lowest order in $\hbar$, it is inevitable at the next order for restoring frame independence of the Wigner function [22,74]. This is a massive generalization of the side-jump effect in the chiral limit [75,76], see also Refs. [39,77]. We note that while it is possible to determine the dynamical part of the axial component of the Wigner function in global equilibrium by principle of frame independence [78], the generalization to the local equilibrium case can be nontrivial. In this paper, we focus on the nondynamical part of the axial component and leave the dynamical part for separate studies.

By solving the constraint equation in (103), we obtain the nondynamical part of both axial and tensor components,

$$S^{<(1)}(P) = \gamma^5\gamma_\mu \mathcal{A}^\mu + \frac{i[\gamma_\mu, \gamma_\nu]}{4} \mathcal{S}^{\mu\nu}, \qquad (104)$$

where

$$\begin{aligned}
\mathcal{A}^\mu &= -2\pi\hbar\epsilon(P\cdot u) \frac{\epsilon^{\mu\nu\rho\sigma} P_\rho u_\sigma \mathcal{D}_\nu f_e}{2(P\cdot u + m)} \delta(P^2 - m^2), \\
\mathcal{S}^{\mu\nu} &= -2\pi\hbar\epsilon(P\cdot u) \frac{\mathcal{D}_{[\mu}P_{\nu]} f_e - m u_{[\mu}\mathcal{D}_{\nu]} f_e - P_{[\mu}u_{\nu]}\mathcal{D}_m}{2(P\cdot u + m)} \\
&\quad \times \delta(P^2 - m^2). \qquad (105)
\end{aligned}$$

The collisional effect is taken into account in the definitions $\mathcal{D}_\nu = \partial_\nu - \Sigma_\nu^> - \Sigma_\nu^< \frac{1-f_e}{f_e}$ and $\mathcal{D}_m = \Sigma_m^> + \Sigma_m^< \frac{1-f_e}{f_e}$ with $\Sigma_\nu^{>/<} = \frac{1}{4}\mathrm{tr}[\Sigma^{>/<}\gamma_\nu]$ and $\Sigma_m^{>/<} = \frac{1}{4}\mathrm{tr}[\Sigma^{>/<}]$. Since $\mathcal{A}^\mu$ gives rise to spin polarization upon frequency integration, see, for example, Ref. [79], the collisional contribution to spin polarization naturally can be readily studied for any given solution to classical kinetic theory.

Let us elaborate on the nature of the $\hbar$ expansion. Recall that in early studies of transport coefficients, $\hbar$ is set to unity, and gradient expansion is used in solving the classical kinetic equation. The gradient expansion of the distribution f reads $f = f_{(0)} + f_{(1)} + \cdots$. Restoring $\hbar$ by dimension, we have $f_{(0)} \sim O(1)$, $f_{(1)} \sim \frac{\hbar\partial_X f_{(0)}}{\Lambda}$. It is clear that the gradient always comes with $\hbar$; therefore, partial corrections at higher order in $\hbar$ are already present in solution to classical kinetic theory. This type of $\hbar$ correction distinguishes from the one discussed above in that the former does not contribute to spin polarization, while the latter does. We still use the terminology classical and quantum as a separation between spin unpolarized and polarized sectors of kinetic theory.

We move on from the quantum correction to the photon Wigner function $D_{\nu\rho}^{<(1)}$ with the same logic in mind. Keeping only the nondynamical equation, we have

$$\begin{aligned}
&\left(-P^2 g^{\mu\nu} + P^\mu P^\nu - \frac{1}{\xi} P^{\mu\alpha} P^{\nu\beta} P_\alpha P_\beta\right) D_{\nu\rho}^{<(1)} \\
&\quad + \frac{i}{2}\bigg(-2P\cdot\partial g^{\mu\nu} + \partial^\mu P^\nu + \partial^\nu P^\mu \\
&\quad - \frac{1}{\xi} P^{\mu\alpha} P^{\nu\beta}(\partial_\alpha P_\beta + \partial_\beta P_\alpha)\bigg) D_{\nu\rho}^{<(0)} \\
&\quad = \frac{i\hbar}{2}(\Pi^{\mu\nu>(0)} D_{\nu\rho}^{<(0)} - \Pi^{\mu\nu<(0)} D_{\nu\rho}^{>(0)}). \qquad (106)
\end{aligned}$$

With the help of the gauge fixing term, we can solve (106) by the following inversion:

$$\left(\frac{u_\mu u_\lambda}{\mathbf{p}^2}+\frac{P^T_{\mu\lambda}}{P^2}-\xi\frac{P_\mu P_\lambda}{\mathbf{p}^4}\right)\left(-P^2g^{\mu\nu}+P^\mu P^\nu-\frac{1}{\xi}P^{\mu\alpha}P^{\nu\beta}P_\alpha P_\beta\right)=\delta^\nu_\lambda, \tag{107}$$

with $\mathbf{p}^2=-P^2+(P\cdot u)^2$. Note that $(\frac{u_\mu u_\lambda}{\mathbf{p}^2}+\frac{P^T_{\mu\lambda}}{P^2}-\xi\frac{P_\mu P_\lambda}{\mathbf{p}^4})$ gives the Coulomb gauge propagator at $\xi=0$. Multiplying it to (106), we obtain

$$\begin{aligned}D^{<(1)}_{\lambda\rho}=&-\left(\frac{u_\mu u_\lambda}{\mathbf{p}^2}+\frac{P^T_{\mu\lambda}}{P^2}-\xi\frac{P_\mu P_\lambda}{\mathbf{p}^4}\right)\frac{i}{2}\Big(-2P\cdot\partial g^{\mu\nu}+\partial^\mu P^\nu\\&+\partial^\nu P^\mu-\frac{1}{\xi}P^{\mu\alpha}P^{\nu\beta}(\partial_\alpha P_\beta+\partial_\beta P_\alpha)\Big)D^{<(0)}_{\nu\rho}\\&+\left(\frac{u_\mu u_\lambda}{\mathbf{p}^2}+\frac{P^T_{\mu\lambda}}{P^2}-\xi\frac{P_\mu P_\lambda}{\mathbf{p}^4}\right)\frac{i\hbar}{2}\\&\times(\Pi^{\mu\nu>(0)}D^{<(0)}_{\nu\rho}-\Pi^{\mu\nu<(0)}D^{>(0)}_{\nu\rho}).\end{aligned}\tag{108}$$

We first show terms $\propto P^T_{\mu\lambda}$ vanish by classical kinetic equations. To see that, we note $D^{</>(0)}_{\nu\rho}\propto P^T_{\nu\rho}$. The only remaining terms on the rhs are

$$\frac{P^T_{\mu\lambda}}{P^2}\frac{i}{2}(2P\cdot\partial g^{\mu\nu}D^{<(0)}_{\nu\rho}+\hbar\Pi^{\mu\nu>(0)}D^{<(0)}_{\nu\rho}-\hbar\Pi^{\mu\nu<(0)}D^{>(0)}_{\nu\rho})\propto P^T_{\lambda\rho}. \tag{109}$$

Since the tensor structure is unique, we can extract its coefficient function by contracting with $P^{\lambda\rho}_T$, which vanishes by the classical kinetic equation. The other terms give the following result in the limit $\xi\to 0$:

$$\begin{aligned}D^{<(1)}_{\lambda\rho}=&-\frac{iu_\lambda(P\cdot u)\partial^\nu D^{<(0)}_{\nu\rho}}{2\mathbf{p}^2}-\frac{iP_\lambda P^{\nu\beta}\partial_\beta D^{<(0)}_{\nu\rho}}{2\mathbf{p}^2}\\&+\frac{i\hbar u_\lambda u_\mu(\Pi^{\mu\nu>(0)}D^{<(0)}_{\nu\rho}-\Pi^{\mu\nu<(0)}D^{>(0)}_{\nu\rho})}{2\mathbf{p}^2}\\=&-\frac{iP_{\lambda\alpha}P^{\nu\beta}P^\alpha\partial_\beta D^{<(0)}_{\nu\rho}}{2\mathbf{p}^2}\\&+\frac{i\hbar u_\lambda u_\mu(\Pi^{\mu\nu>(0)}D^{<(0)}_{\nu\rho}-\Pi^{\mu\nu<(0)}D^{>(0)}_{\nu\rho})}{2\mathbf{p}^2}.\end{aligned}\tag{110}$$

In the second line, we have used $\partial^\nu D^{<(0)}_{\nu\rho}=-P^{\nu\beta}\partial_\beta D^{<(0)}_{\nu\rho}$. However, (110) cannot be the correct quantum correction to the Wigner function. Since $D^<_{\nu\rho}$ is Hermitian, a purely imaginary $D^{<(1)}_{\nu\rho}$ in (110) indicates it should be antisymmetric in indices [65], which is obviously not satisfied by (110). The resolution is simple; since we consider on-shell photons, the operator $-P^2g^{\mu\nu}+P^\mu P^\nu-\frac{1}{\xi}P^{\mu\alpha}P^{\nu\beta}P_\alpha P_\beta$ contains a zero mode. Equation (110) can be modified by a zero mode contribution. We can make (110) Hermitian by adding its own Hermitian conjugate,

$$D^{<(1)}_{\lambda\rho}=\frac{iP_{\rho\alpha}P^{\nu\beta}P^\alpha\partial_\beta D^{<(0)}_{\nu\lambda}}{2\mathbf{p}^2}+\frac{i\hbar u_\rho u_\mu(\Pi^{\mu\nu>(0)}D^{<(0)}_{\nu\lambda}-\Pi^{\mu\nu<(0)}D^{>(0)}_{\nu\lambda})}{2\mathbf{p}^2}. \tag{111}$$

It turns out (111) is at the same time a zero mode of $-P^2g^{\mu\nu}+P^\mu P^\nu-\frac{1}{\xi}P^{\mu\alpha}P^{\nu\beta}P_\alpha P_\beta$ using $D^{<(0)}_{\nu\lambda}\propto P^T_{\nu\lambda}\delta(P^2)$. Adding up (110) and (111), we find the quantum correction,[10]

$$\begin{aligned}D^{<(1)}_{\lambda\rho}=&-\frac{iP_{\lambda\alpha}P^{\nu\beta}P^\alpha\partial_\beta D^{<(0)}_{\nu\rho}}{2(-P^2+(P\cdot u)^2)}+\frac{i\hbar u_\lambda u_\mu(\Pi^{\mu\nu>(0)}D^{<(0)}_{\nu\rho}-\Pi^{\mu\nu<(0)}D^{>(0)}_{\nu\rho})}{2(-P^2+(P\cdot u)^2)}-(\lambda\leftrightarrow\rho)\\=&-2\pi\epsilon(P\cdot u)\delta(P^2)\frac{iP_{\lambda\alpha}P^{\nu\beta}P^\alpha\partial_\beta P^T_{\nu\rho}f_\gamma(P)}{2(-P^2+(P\cdot u)^2)}+2\pi\epsilon(P\cdot u)\delta(P^2)P^T_{\nu\rho}\\&\times\frac{i\hbar u_\lambda u_\mu(\Pi^{\mu\nu>(0)}f_\gamma(P)-\Pi^{\mu\nu<(0)}(1+f_\gamma(P)))}{2(-P^2+(P\cdot u)^2)}-(\lambda\leftrightarrow\rho).\end{aligned}\tag{112}$$

In the collisionless limit, (112) agrees with [65]. To see the equivalence, we note that the counterpart in [65] can be obtained by replacing $P^T_{\nu\rho}$ in the first term by $P_{\nu\rho}$. The difference from the replacement is proportional to

$$P_{\lambda\alpha}P^\alpha P_\mu P^{\mu\beta}\partial_\beta P_{\rho\sigma}P^\sigma-(\lambda\leftrightarrow\rho), \tag{113}$$

which vanishes identically by the antisymmetrization in indices. Equation (112) also contains a collisional contribution, which has the form of $\Pi^{\mu\nu}$ sandwiched between $u_\lambda u_\mu$ and $P^T_{\nu\rho}$. In an isotropic medium, $\Pi^{\mu\nu}=P^{\mu\nu}_L\Pi_L+P^{\mu\nu}_T\Pi_T$, so this contribution vanishes identically by the orthogonality condition of the projectors. In a generic off-equilbrium medium, for example, one with a shear gradient, more structures are allowed in the self-energy, so the collisional contribution is, in general, nonvanishing. Unlike in the case

[10] The appearance of a factor of $\hbar$ is consistent with the dimension of photon self-energy $\Pi^{\mu\nu}(P)\sim\text{length}^{-2}$.

of screening, the effect of the gradient on the quantum correction here is leading order.

VI. OUTLOOK

We have derived a quantum kinetic theory for QED by assuming parity invariance. At lowest order in $\hbar$, it generalizes well-known classical kinetic theory to the massive case. We have also found a nondynamical quantum correction to the Wigner function at $O(\hbar)$, which gives the spin polarization of fermions and photons. Several interesting extensions of this work can be studied.

First of all, relaxing the parity invariant constraint would introduce more degrees of freedom to kinetic theory. It makes the distribution functions spin dependent, allowing us to study the spin evolution within kinetic theory. These are of particular interest in the physics-like chiral magnetic effect, in which local parity violation is also present.

Secondly, the notion of locality can be further explored in kinetic theory. We have different scales for collisions with $1/e^2\Lambda$ corresponding to the effective range of inelastic collisions and $1/e\Lambda$ corresponding to the range of elastic collisions. In our case, both are local because of our larger coarse-graining scale $1/e^4\Lambda$. It would be interesting to look at other possibilities; for example, choosing $1/e\Lambda$ as a coarse-graining scale would lead to nonlocal inelastic collisions, allowing us to study the transfer between orbital and spin angular momenta. With this finer notion of locality, we also need to take into account the electromagnetic field from fluctuations.

Finally, it is clearly desirable to extend the present study to a QCD case and determine the corresponding spin transport coefficients. This would shed light on the applicability of spin hydrodynamics in the system of spinning quark-gluon plasma-produced heavy ion collisions.

ACKNOWLEDGMENTS

We are grateful to Wei-jie Fu, Jian-hua Gao, Defu Hou, Shi Pu, Xin-li Sheng, and Ziyue Wang for useful discussions. We are also grateful to the anonymous referee for insightful criticisms on earlier versions of the paper. This work is in part supported by NSFC under Grants No. 12075328, No. 11735007, and No. 11675274.

APPENDIX A: FROM SELF-ENERGIES TO COLLISION TERMS

In this Appendix, we show how (43), (44), (45), (46), (47), and (48) can be reduced to collision terms in the Boltzmann equation for QED.

We start with (43) and focus on the case $p_0 > 0$, i.e., fermion in the initial state. The case $p_0 < 0$ can be deduced by crossing symmetry. There are in total eight ways in choosing the sign of k_0, k_0', and p_0'. Only the following three are kinematically allowed: $k_0 > 0$, $k_0' > 0$, $p_0' > 0$; $k_0 < 0$, $k_0' < 0$, $p_0' > 0$; and $k_0 < 0$, $k_0' > 0$, $p_0' < 0$. The second and third cases are related to the first one by crossing symmetry. Let us consider the first case. The kinematical region implies it corresponds to the square of the s-channel Compton. To see that, we use

$$P^T_{\nu\mu}(K) = \sum_i \epsilon^i_\nu(K)\epsilon^{i*}_\mu(K), \tag{A1}$$

and similarly for $P^T_{\sigma\rho}(K')$, which relates the projector to sum over the initial/final states of photons. We can further use the spin sum formula for $\not{P} + m$ from $S^<(P)$,

$$\not{P} + m = \sum_s u_s(P)\bar{u}_s(P), \tag{A2}$$

and similarly for $\not{P}' + m$ from $S^>(P')$. Recall in Sec. II that trace ise taken in deriving the dynamical equation for f_e. With all the rewritings above and cyclic property of the trace, we have from tr[(33)],[11]

$$\begin{aligned}\sum_{s,t,i,j} &\mathrm{tr}[\bar{u}_s(P)\gamma^\mu S_{11}(K+P)\gamma^\rho u_t(P')\epsilon^i_\sigma(K')\epsilon^j_\mu(K)\bar{u}_t(P') \\ &\times \gamma^\sigma S_{22}(K+P)\gamma^\nu u_s(P)\epsilon^{i*}_\rho(K')\epsilon^{j*}_\nu(K)] \\ &\times f_e(P)f_\gamma(K)(1-f_e(P'))(1+f_\gamma(K'))\delta(P^2)\delta(P'^2) \\ &\times \delta(K^2)\delta(K'^2),\end{aligned} \tag{A3}$$

which is clearly identified as the square of the s-channel Compton scattering. By crossing symmetry, we obtain the square of the t-channel Compton scattering and t-channel annihilation for the other two cases. The action of crossing symmetry on distribution functions use the constraints $f_e(P) + f_e(-P) = 1$ and $f_\gamma(P) + f_\gamma(-P) = 1$ to convert distribution functions of particles to those of antiparticles.

Equation (44) can be rewritten similarly. For the cases $p_0 > 0$, $k_0 > 0$, $k_0' > 0$, and $p_0' > 0$, we also use (A1) and (A2) to rewrite tr[(44)] as

$$\begin{aligned}\sum_{s,t,i,j} &\mathrm{tr}[\bar{u}_s(K')\gamma^\beta u_t(P')\bar{u}_t(P')\gamma^\alpha u_s(K')]\mathrm{tr}[\bar{u}_i(P)\gamma^\mu u_j(K) \\ &\times \bar{u}_j(K)\gamma^\nu u_i(P)]D^{11}_{\nu\alpha}(K-P) \\ &\times D^{22}_{\beta\mu}(K-P)f_e(P)f_e(P')(1-f_e(K))(1-f_e(K')) \\ &\times \delta(P^2)\delta(P'^2)\delta(K^2-m^2)\delta(K'^2-m^2),\end{aligned} \tag{A4}$$

which corresponds to the square of the t-channel Coulomb scattering between fermions. By crossing symmetry, we can obtain also the squares of s-/t-channels Coulomb scattering between fermions and antifermions.

Now, we turn to (45). In fact, tr[(43)] and (45) are simply related by relabeling of momenta $P \leftrightarrow K$. It follows that (45) also corresponds to squares of s-/t-channels Compton scattering and t-channel annihilation.

[11]An overall numerical factor $(2\pi)^4$ is suppressed.

The identification with interference terms proceeds similarly. For the vertex correction to photon self-energy (46), we can use the cyclic property of the trace to rewrite (46) up to overall factors of $f_\gamma(P)f_e(P')(1-f_e(K))(1+f_\gamma(K'))\delta(P^2)\delta(P'^2)\delta(K^2-m^2)\delta(K'^2-m^2)$ as

$$\sum_{s,t,i,j}\mathrm{tr}[\bar{u}_s(K)\gamma^\mu S_{22}(P-K)\gamma^\rho u_t(P')]\epsilon^i_\rho(Q)\epsilon^{j*}_\mu(P)\times\mathrm{tr}[\bar{u}_t(P')\gamma^\nu S_{11}(P+P')\gamma^\sigma u_s(K)]\epsilon^{i*}_\sigma(Q)\epsilon^j_\nu(P)$$
$$=\sum_{s,t,i,j}(\mathrm{tr}[\bar{u}_t(P')\gamma^\rho S_{11}(P-K)\gamma^\mu u_s(K)]\epsilon^{i*}_\rho(Q)\epsilon^j_\mu(P))^*\times\mathrm{tr}[\bar{u}_t(P')\gamma^\nu S_{11}(P+P')\gamma^\sigma u_s(K)]\epsilon^{i*}_\sigma(Q)\epsilon^j_\nu(P). \quad (A5)$$

This is the product of the s-channel amplitude with the complex conjugate of the t-channel amplitude for Compton scattering, to be abbreviated st^* of Compton. By crossing symmetry, we can easily obtain the s^*t of Compton and t^*u of annihilation. Note that we have only half of the interference terms for annihilation.

For the vertex correction to fermion self-energy, we look at (47) first. Using (21), we have

$$S^>(-P')=\bar{S}^<(P'). \quad (A6)$$

Note that $\bar{S}$ has the sign of mass flipped. We can represent the corresponding Dirac structure by the spin sum of antifermions,

$$\not{P}'-m=\sum_s v_s(P')\bar{v}_s(P'). \quad (A7)$$

We can then rewrite the trace of (47) up to $f_e(P)f_e(P')(1+f_\gamma(K))(1+f_\gamma(K'))\delta(P^2-m^2)\delta(P'^2-m^2)\delta(K^2)\delta(K'^2)$ as

$$\sum_{s,t,i,j}\mathrm{tr}[\bar{u}_s(P)\gamma^\mu S_{22}(P-K)\gamma^\nu v_t(P')]\epsilon_\mu(K)\epsilon^*_\nu(K')\times\mathrm{tr}[\bar{v}_t(P')\gamma^\rho S_{11}(P-K')\gamma^\sigma u_s(P)]\epsilon^*_\rho(K)\epsilon_\sigma(K')$$
$$=\sum_{s,t,i,j}(\mathrm{tr}[\bar{v}_t(P')\gamma^\nu S_{11}(P-K)\gamma^\mu u_s(P)]\epsilon^*_\mu(K)\epsilon_\nu(K'))^*\times\mathrm{tr}[\bar{v}_t(P')\gamma^\rho S_{11}(P-K')\gamma^\sigma u_s(P)]\epsilon^*_\rho(K)\epsilon_\sigma(K'), \quad (A8)$$

which corresponds to half of the interference term of annihilation. By crossing symmetry, we can obtain interference terms of Compton scattering.

Finally, we turn to (48), which has slightly different momenta labeling from the other cases, with P, P', $P-K$, and $P-K'$ on shell instead. We consider the kinematical region with $p_0'<0$, $p_0-k_0>0$, $p_0-k_0'>0$. Using the similar procedure as before, we rewrite (48) up to overall factors of $f_e(P)f_e(P')(1+f_\gamma(P-K))(1+f_\gamma(P-K'))\times\delta(P^2-m^2)\delta(P'^2-m^2)\delta((P-K)^2-m^2)\delta((P-K')^2-m^2)$ as

$$\sum_{s,t,i,j}\mathrm{tr}[\bar{u}_s(P)\gamma^\mu u_t(P-K)]\mathrm{tr}[\bar{u}_i(-P')\gamma^\rho u_j(P-K')]D^{22}_{\mu\rho}(K)\mathrm{tr}[\bar{u}_t(P-K)\gamma^\nu u_i(-P')]\mathrm{tr}[\bar{u}_j(P-K')\gamma^\sigma u_s(P)]D^{11}_{\nu\sigma}(K')$$
$$=\sum_{s,t,i,j}(\mathrm{tr}[\bar{u}_t(P-K)\gamma^\mu u_s(P)]\mathrm{tr}[\bar{u}_j(P-K')\gamma^\rho u_i(-P')]D^{11}_{\mu\rho}(K))^*\mathrm{tr}[\bar{u}_t(P-K)\gamma^\nu u_i(-P')]\mathrm{tr}[\bar{u}_j(P-K')\gamma^\sigma u_s(P)]D^{11}_{\nu\sigma}(K'). \quad (A9)$$

This gives the product of t-channel amplitude with the complex conjugate of u-channel amplitude of Coulomb scattering between fermions (tu^*). By crossing symmetry, we can also obtain st^* and s^*t of Coulomb scattering between fermions and antifermions.

APPENDIX B: EVALUATION OF SELF-ENERGIES

In this Appendix, we evaluate the retarded self-energies of fermions and photons, which are needed for determination of thermal masses in the main text. The retarded self-energies have the following representations in ra basis: $S_R=iS_{ra}$ and $D^R_{\mu\nu}=iD^{ra}_{\mu\nu}$, which allows us to perform the calculation in ra basis.

We first evaluate the fermion self-energy, which we need in two different kinematical regions: soft off-shell momenta (for screening effect in elastic collisions) and hard on-shell momenta (for inelastic collisions). In both cases, we also require $m\lesssim e\Lambda$ in order for screening or inelastic collisions to be relevant. This condition allows us to drop m in the evaluation of fermion self-energy. It is known from explicit calculations that the fermion self-energies in equilibrium are the same in Coulomb gauge [64] and Feynman gauge [80]. The agreement is expected to hold for the off-equilibrium case at the lowest order because the structures of propagators do not change from the equilibrium case to the off-equilibrium case. Below, we proceed in the Feynman gauge. Figure 9 shows the self-energy diagrams in ra basis, which give

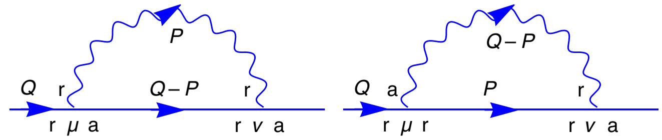

FIG. 9. One-loop fermion self-energy Σ_{ra}. Vertices can have labelings rra and aaa.

$$\Sigma_{ra}(Q) = -e^2 \int_P \gamma^\mu S_{ar}(Q-P)\gamma^\nu D^{rr}_{\nu\mu}(P) - e^2 \int_P \gamma^\mu S_{rr}(P)\gamma^\nu D^{ar}_{\nu\mu}(Q-P). \tag{B1}$$

The relevant propagators in ra basis are given by

$$S_{ar}(P) = \frac{i(\not{P}+m)}{(p_0-i\epsilon)^2 - p^2 - m^2},$$
$$S_{rr}(P) = \left(\frac{1}{2} - f_e(P)\right)(\not{P}+m)2\pi\epsilon(p_0)\delta(P^2-m^2),$$
$$D^{ar}_{\mu\nu}(P) = \frac{-ig_{\mu\nu}}{(p_0-i\epsilon)^2 - p^2},$$
$$D^{rr}_{\mu\nu}(P) = -g_{\mu\nu}\left(\frac{1}{2}+f_\gamma(P)\right)2\pi\epsilon(p_0)\delta(P^2).$$

As we argued above, we can drop m in S_{ar} and S_{rr}. Furthermore, we can drop Q^2 in the denominators of $S_{ar}(Q-P)$ and $D^{ar}_{\nu\mu}(Q-P)$, because either Q is soft off-shell $Q^2 \ll Q\cdot P$ or hard on-shell $Q^2 = 0$. We thus have

$$i\Sigma_{ra}(Q) = -e^2 \int_P \frac{-2(\not{Q}-\not{P})}{-2P\cdot Q}\left(\frac{1}{2}+f_\gamma(P)\right)2\pi\epsilon(p_0)\delta(P^2) - e^2 \int_P \frac{-2\not{P}}{-2P\cdot Q}\left(\frac{1}{2}-f_e(P)\right)2\pi\epsilon(p_0)\delta(P^2), \tag{B2}$$

where we have dropped $i\epsilon$ in the denominators because $Q-P$ is of -shell. Separating the cases of particles and antiparticles, we can expand (B2) as

$$\begin{aligned} i\Sigma_{ra}(Q) = &-e^2 \int \frac{d^3p}{(2\pi)^3}\frac{1}{2p}\left(\frac{-2(\not{Q}-\not{P})}{-2P\cdot Q}\left(\frac{1}{2}+f_\gamma(\vec{p})\right) - \frac{-2(\not{Q}-\bar{\not{P}})}{-2\bar{P}\cdot Q}\left(\frac{1}{2}-f_\gamma(-\vec{p})\right)\right) \\ &- e^2 \int \frac{d^3p}{(2\pi)^3}\frac{1}{2p}\left(\frac{-2\not{P}}{-2P\cdot Q}\left(\frac{1}{2}-f_e(\vec{p})\right) - \frac{-2\bar{\not{P}}}{-2\bar{P}\cdot Q}\left(-\frac{1}{2}-f_{\bar{e}}(-\vec{p})\right)\right), \end{aligned} \tag{B3}$$

where $\bar{P} = (-p_0, \vec{p})$, and $f_{\bar{e}}$ is the distribution function of antifermions defined below (35). We can then use a change in variable $\vec{p} \to -\vec{p}$ to arrive at

$$\begin{aligned} i\Sigma_{ra}(Q) = &-e^2 \int \frac{d^3p}{(2\pi)^3}\frac{1}{2p}\left(\frac{-2(\not{Q}-\not{P})}{-2P\cdot Q}\left(\frac{1}{2}+f_\gamma(\vec{p})\right) - \frac{-2(\not{Q}+\not{P})}{2P\cdot Q}\left(-\frac{1}{2}-f_\gamma(\vec{p})\right)\right) \\ &- e^2 \int \frac{d^3p}{(2\pi)^3}\frac{1}{2p}\left(\frac{-2\not{P}}{-2P\cdot Q}\left(\frac{1}{2}-f_e(\vec{p})\right) - \frac{2\not{P}}{2P\cdot Q}\left(\frac{1}{2}+f_{\bar{e}}(\vec{p})\right)\right). \end{aligned} \tag{B4}$$

Dropping the $\frac{1}{2}$ in the brackets, which correspond to the vacuum contributions, we end up with

$$i\Sigma_{ra}(Q) = e^2 \int \frac{d^3p}{(2\pi)^3}\frac{1}{2p}\frac{\not{P}}{P\cdot Q}(2f_\gamma(\vec{p}) + f_e(\vec{p}) + f_{\bar{e}}(\vec{p})). \tag{B5}$$

Since we require $m \lesssim e\Lambda$, and Q can be either hard on shell or soft off shell, including the mass in the evaluation of fermion self-energy would only lead to a correction at order $O(e^3\Lambda^2/Q)$.

Next, we turn to the retarded photon self-energy, which we also need in two different kinematical regions: soft off-shell momenta (for screening in elastic collisions) and hard on-shell momenta (for inelastic collisions). However, there is one small difference from the fermion self-energy. While in the case of inelastic collisions photon self-energy is never needed for very massive fermion $m \gg e\Lambda$ because this would make inelastic scattering itself irrelevent, it is always needed for screening in elastic collisions for arbitrary fermion mass. So we do not drop m as in the following evaluation of photon self-energy, since the photon self-energy at leading order in coupling is gauge invariant. We can also evaluate it in Feynman gauge. The corresponding diagrams are shown in Fig. 10, which give

$$\begin{aligned} \Pi^{ra}_{\mu\nu} &= e^2 \int_P \mathrm{tr}[\gamma^\mu S_{rr}(P)\gamma^\nu S_{ra}(P-Q)] + e^2 \int_P \mathrm{tr}[\gamma^\mu S_{ar}(P)\gamma^\nu S_{rr}(Q-P)] \\ &= e^2 \int_P \mathrm{tr}[\gamma^\mu S_{rr}(P)\gamma^\nu S_{ra}(P-Q)] + (Q \to -Q, \mu \leftrightarrow \nu). \end{aligned} \tag{B6}$$

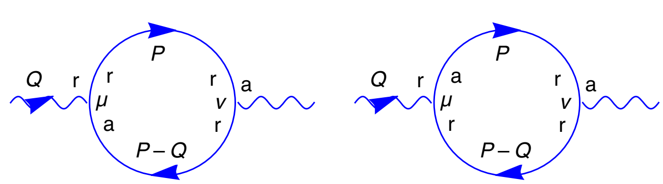

FIG. 10. One-loop hard photon self-energy Π_{ra}. Vertices can have labelings rra and aaa.

The contribution from the second diagram is related the counterpart from the first one by the replacement $Q \to -Q$, $\mu \leftrightarrow \nu$. This can be shown by using the property $S_{ar}(P) = S_{ra}(P)$ which is valid for off-shell momentum and relabeling of momentum $P \to Q - P$. Keeping fermion mass in the propagators for the photonic case, we evaluate the trace as

$$\mathrm{tr}[\gamma^\mu(\not{P}+m)\gamma^\nu(\not{P}-\not{Q}+m)] = 8P^\mu P^\nu - 4(P^\mu Q^\nu + P^\nu Q^\mu) + 4g^{\mu\nu}P\cdot Q. \tag{B7}$$

Note that the m dependence drops by the on-shell condition of P. It turns out that the leading contribution from the term $P^\mu P^\nu$ vanishes upon combination of the two diagrams; thus, we cannot simply drop the Q^2 in $S_{ra}(P-Q)$ as in the fermionic case. Instead, we should approximate $S_{ra}(P-Q)$ as

$$S_{ra}(P-Q) \simeq \frac{i(\not{P}-\not{Q}+m)}{-2P\cdot Q}\left(1+\frac{Q^2}{2P\cdot Q}\right). \tag{B8}$$

The remaining evaluation is similar. In the end, we find two diagrams contribute equally to give

$$i\Pi^{ra}_{\mu\nu}(Q) = 2e^2\int\frac{d^3p}{(2\pi)^3}\frac{1}{E_p}(f_e(\vec{p})+f_{\bar{e}}(\vec{p})) \times\left[\frac{P_\mu Q_\nu + P_\nu Q_\mu - g_{\mu\nu}P\cdot Q}{P\cdot Q} - \frac{P^\mu P^\nu Q^2}{(P\cdot Q)^2}\right], \tag{B9}$$

with $E_p = \sqrt{p^2+m^2}$. The Ward identity can be verified as

$$iQ^\mu\Pi^{ra}_{\mu\nu}(Q) = 0. \tag{B10}$$

Finally, we calculate the self-energy $\Pi^{aa}_{\mu\nu}$ for the soft photon, which is used to determine $D^{rr}_{\mu\nu}$. In this case, we also have $m \lesssim e\Lambda$ so that inelastic collisions are relevant. $\Pi^{aa}_{\mu\nu}$ contains contributions from three diagrams in Fig. 11. Only the last one is medium dependent, which gives

$$\Pi^{aa}_{\mu\nu}(Q) = e^2\int_{P,P'}(2\pi)^4\delta(P-P'-Q)\mathrm{tr}[\gamma_\mu\not{P}\gamma_\nu\not{P}'] \times 2\pi\epsilon(p_0)\delta(P^2)\left(\frac{1}{2}-f_e(P)\right) \times 2\pi\epsilon(p'_0)\delta(P'^2)\left(\frac{1}{2}-f_e(P')\right). \tag{B11}$$

Note that we have dropped mass in the propagators. For $Q \ll P, P'$, p_0 and p'_0 have the same sign; thus, $\epsilon(p_0)\epsilon(p'_0) = 1$. We expand the delta functions and evaluate the trace to obtain

$$\begin{aligned}\Pi^{aa}_{\mu\nu}(Q) = e^2\int\frac{d^3p}{(2\pi)^3}\frac{1}{4pp'}(2\pi)\delta(p-|\mathbf{p}-\mathbf{q}|-q_0) &\times\Big[(4P_\mu P'_\nu + 4P_\nu P'_\mu - 4g_{\mu\nu}P\cdot P')\\ &\times\left(\frac{1}{2}-f_e(\vec{p})\right)\left(\frac{1}{2}-f_e(\vec{p}')\right)\\ &+(4\bar{P}_\mu\bar{P}'_\nu + 4\bar{P}_\nu\bar{P}'_\mu - 4g_{\mu\nu}\bar{P}\cdot\bar{P}')\\ &\times\left(\frac{1}{2}-f_{\bar{e}}(-\vec{p})\right)\left(\frac{1}{2}-f_{\bar{e}}(-\vec{p}')\right)\Big].\end{aligned} \tag{B12}$$

We further approximate $P'_\mu \simeq P_\mu$, $\bar{P}'_\mu \simeq \bar{P}_\mu$ and neglect $P\cdot P' = -Q^2 + 2m^2$. Finally, we make a change of variable $\vec{p} \to -\vec{p}$. It amounts to the replacement $\bar{P} \to -P$ and $f_{\bar{e}}(-\vec{p}) \to f_{\bar{e}}(\vec{p})$, after which we obtain

$$\Pi^{aa}_{\mu\nu} = e^2\int\frac{d^3p}{(2\pi)^3}2\hat{P}_\mu\hat{P}_\nu(2\pi) \times\delta(p-|\mathbf{p}-\mathbf{q}|-q_0)(f_e(\vec{p})^2 - f_e(\vec{p})) + (f_e \to f_{\bar{e}}), \tag{B13}$$

with $\hat{P}^\mu = (1, \hat{p})$.

To determine $D^{rr}_{\mu\nu}$, we use the following identities:

$$D^{rr}_{\mu\nu} = \frac{1}{2}(D^>_{\mu\nu} + D^<_{\mu\nu}),\quad \Pi^{aa}_{\mu\nu} = \frac{1}{2}(\Pi^>_{\mu\nu} + \Pi^<_{\mu\nu}). \tag{B14}$$

Using $D^{</>}_{\mu\nu} = -D^R_{\mu\alpha}\Pi^{\alpha\beta</>}D^A_{\beta\nu} + O(\hbar)$, we obtain

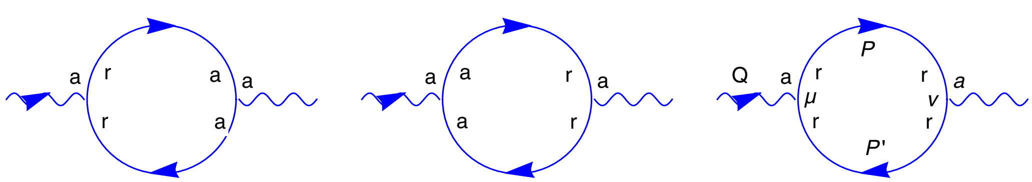

FIG. 11. One-loop soft photon self-energy Π_{aa}. Vertices can have labelings rra and aaa. Only the third diagram is medium dependent.

$$D^{rr}_{\mu\nu} = -D^R_{\mu\alpha}\Pi^{\alpha\beta}_{aa}D^A_{\beta\nu}, \tag{B15}$$

where D^R is given by (58) and D^A determined from (52).

APPENDIX C: DAMPING RATE OF HARD FERMION

The damping rate Γ is determined from the dispersion $p_0 = E_p - \frac{i\Gamma}{2}$, which is the root of the following equation:

$$(P_\mu - \Sigma^R_\mu)^2 - (m - \Sigma^R_m)^2 = 0, \tag{C1}$$

with $\Sigma^R = \Sigma^R_\mu\gamma^\mu + \Sigma^R_m 1$. It is the same equation as (63), but now we need to find out the imaginary part of p_0. Note that $\Sigma^R_\mu \sim e^2$ and $\Sigma^R_m = 0$ to the order of our interest. From (C1), we obtain

$$\Gamma = -\frac{1}{2p_0}\mathrm{Im}(\mathrm{tr}[\not{P}\Sigma^R]) = -\frac{1}{2p_0}\mathrm{Re}(\mathrm{tr}[\not{P}\Sigma^{ra}]). \tag{C2}$$

We proceed with the following representation from the left panel of Fig. 9 (with P and Q exchanged):

$$\Sigma^{ra}(P) = -e^2\int_Q \gamma^\mu S_{ar}(P-Q)\gamma^\nu D^{rr}_{\nu\mu}(Q). \tag{C3}$$

Plugging (C3) into (C2) and using that $D^{rr}_{\mu\nu}$ is real, we obtain

$$\mathrm{Re}(\mathrm{tr}[\not{P}\Sigma^{ra}]) = -e^2\int_Q \mathrm{Re}\left(\mathrm{tr}[\not{P}\gamma^\mu(\not{P}-\not{Q})\gamma^\nu]\frac{i}{(p_0-q_0-i\epsilon)^2-(|\mathbf{p}-\mathbf{q}|)^2-m^2}\right)D^{rr}_{\nu\mu}(Q). \tag{C4}$$

Since $Q \ll P$, we can approximate $\mathrm{tr}[\not{P}\gamma^\mu(\not{P}-\not{Q})\gamma^\nu] \simeq 8P^\mu P^\nu$ and take the real part as

$$\begin{aligned}&\mathrm{Re}\left(\frac{i}{(p_0-q_0-i\epsilon)^2-(|\mathbf{p}-\mathbf{q}|)^2-m^2}\right)\\ &\quad\simeq \mathrm{Re}\left(\frac{i}{2p_0q_0-2\vec{p}\cdot\vec{q}-p_0 i\epsilon}\right)\\ &\quad= \delta(2p_0q_0-2\vec{p}\cdot\vec{q})\epsilon(p_0) = \frac{\pi}{2p_0}\delta(q_0-q_\parallel),\end{aligned} \tag{C5}$$

where $q_\parallel = \vec{q}\cdot\hat{p}$. In the end, we have

$$\Gamma = e^2\int\frac{d^3q}{(2\pi)^3}\hat{P}^\mu\hat{P}^\nu D^{rr}_{\nu\mu}(Q). \tag{C6}$$

Since Q is soft, the suppression factor e^3 from phase space d^3q is compensated by the Bose enhanced propagator $D^{rr}\sim e^{-3}$, giving $\Gamma\sim e^2$. Such an enhancement mechanism is not present in the contribution from the right panel of Fig. 9, so we ignore it.

APPENDIX D: RELATING FOUR-POINT CORRELATORS IN 12 AND *ra* BASIS

The lesser and greater photon self-energies require knowledge of fermion four-point correlators in the 12 basis, while we calculate in Sec. IV only one particular correlator in the *ra* basis. In this Appendix, we establish a relation between them. The fermion four-point correlator is defined as

$$G_{ijkl}(x,x',y,y') = \langle\psi_i(x)\bar{\psi}_k(y)\psi_l(y')\bar{\psi}_j(x')\rangle, \tag{D1}$$

with labels taking values either in 12 or in *ra* basis. Using the basic relation between field in different basis,

$$\psi_r = \frac{1}{2}(\psi_1+\psi_2), \qquad \psi_a = \psi_1-\psi_2, \tag{D2}$$

and we easily obtain

$$\begin{aligned}G_{1122} = {}& G_{rrrr} + \frac{1}{2}G_{rarr} + \frac{1}{2}G_{arrr} - \frac{1}{2}G_{rrar} - \frac{1}{2}G_{rrra}\\ &+ \frac{1}{4}G_{aarr} + \frac{1}{4}G_{rraa} + \cdots,\end{aligned} \tag{D3}$$

with $\cdots$ including correlators with at least three a's in *ra* basis. They are not allowed in the pinching kinematical region.[12] Note that we have calculated G_{aarr}. The other labelings appearing in (D3) can be simply related to G_{aarr} as we now set out to find.

From the diagrammatic representations in Fig. 12, we easily deduce using $S^{rr} = (S^{ra}-S^{ar})(\frac{1}{2}-f_e)$,

$$\begin{aligned}G_{rarr} &= -\left(\frac{1}{2}-f_e(P+K)\right)G_{aarr},\\ G_{rrra} &= \left(\frac{1}{2}-f_e(P+K)\right)G_{rraa},\\ G_{arrr} &= \left(\frac{1}{2}-f_e(P)\right)G_{aarr},\\ G_{rrar} &= -\left(\frac{1}{2}-f_e(P)\right)G_{rraa},\end{aligned} \tag{D4}$$

[12]This is because in these cases at least one end is labeled by two a's; then, the opposite end is forced to have two r's, contradicting the assumed number of a's.

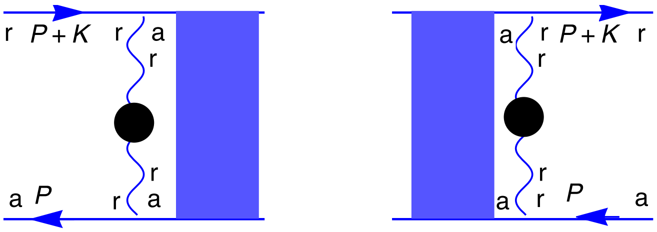

FIG. 12. Labelings for G_{rarr} and G_{rrra}. With the pinching mechanism, the labels are uniquely fixed. G_{arrr} and G_{rrar} can be obtained by exchanging r and a on one end. The shaded structures correspond to G_{aarr} (left panel) and G_{rraa} (right panel), respectively.

where we have extracted relevant components of S^{rr} in arriving at the above. For example, we keep S^{ar} in G_{rarr} dropping S^{ra} because it is paired with another S_{ra}. G_{rrrr} is a little complicated. We claim that contributions containing alternating propagators like $\binom{S_{ra}(P+K)\; S_{ar}(P+K)}{S_{ar}(P)\quad S_{ra}(P)}$ all vanish. We show below such a contribution cancel among different diagrams. Referring to Fig. 13, we see the that alternating contribution can arise from four possible subdiagrams. Extracting the proportionality function of $\binom{S_{ra}(P+K)\; S_{ar}(P+K)}{S_{ar}(P)\quad S_{ra}(P)}$, we have

$$2\left(\frac{1}{2}-f_e(P)\right)\left(\frac{1}{2}-f_e(P+K)\right) -2\left(\frac{1}{2}-f_e(P)\right)\left(\frac{1}{2}-f_e(P+K)\right)=0. \tag{D5}$$

Therefore, only nonalternating contributions are allowed, which are either G_{aarr} or G_{rraa}. It follows that

$$\begin{aligned} G_{rrrr} &= -\left(\frac{1}{2}-f_e(P)\right)\left(\frac{1}{2}-f_e(P+K)\right)(G_{aarr}+G_{rraa}) \\ &= -\left(\frac{1}{2}-f_e(P)\right)\left(\frac{1}{2}-f_e(P+K)\right)2\mathrm{Re}(G_{rraa}), \end{aligned} \tag{D6}$$

where we have used $G_{rraa}=G^*_{aarr}$. A similar analysis gives

$$G_{2211}=f_e(P)(1-f_e(P+K))2\mathrm{Re}G_{aarr}. \tag{D7}$$

They are off-equilibrium generalizations of KMS relations in [81] in the special pinching kinematical region.

APPENDIX E: FERMION SELF-ENERGIES WITH BOTH VERTICES RESUMMED

In this Appendix, we show that fermion self-energies with both vertices resummed is not allowed. We work in the ra basis. Recall from the previous Appendix that all the nonvanishing four-point correlators can be generated from the two basic ones G_{aarr} and G_{rraa} by flipping labels from a to r. We show in Fig. 14 three inequivalent diagrams with two vertices constructed using G_{aarr} and G_{rraa}. Other diagrams can be generated from them by flipping labels. Since labels can only be flipped from a to r, we find diagrams in the top row, and those with labels flipped always contain at least an aa propagator for either fermion or photon and thus are not allowed. In the bottom row, we do find a possible flipping without aa propagators. However, this diagram contains the pair of propagators $S_{ar}(P+K)D^{\mu\nu}_{ar}(K)\sim D_{ar}(P+K)D_{ar}(K)$, which vanish identically upon integration of k_0 by closing the contour properly.

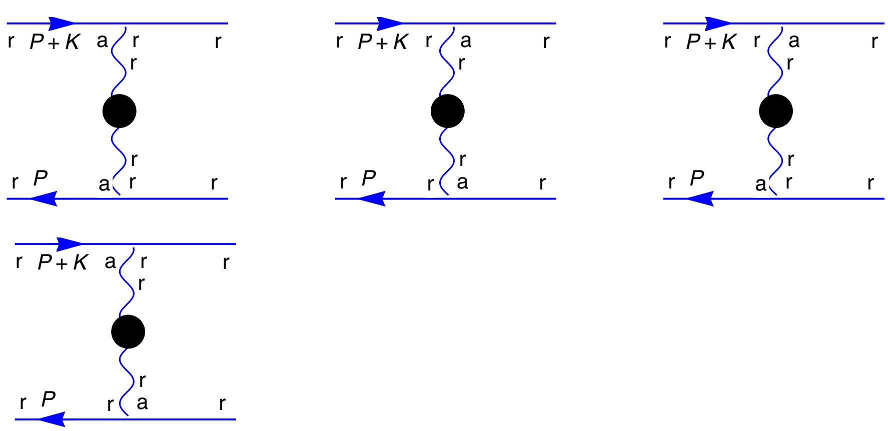

FIG. 13. Possible subdiagrams contributing to alternating unit $\binom{S_{ra}(P+K)\; S_{ar}(P+K)}{S_{ar}(P)\quad S_{ra}(P)}$. Note that the labels for the part extending from both sides of the subdiagrams are uniquely fixed.

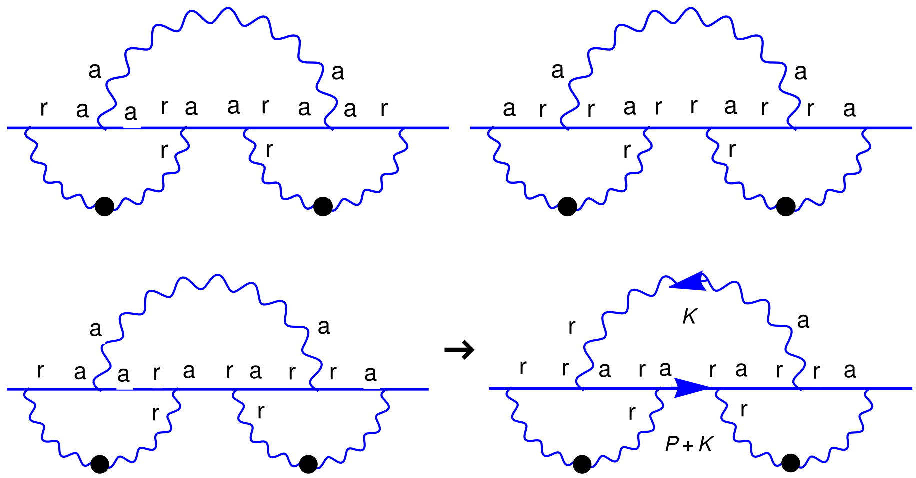

FIG. 14. The top row shows self-energy diagrams with both vertices constructed from G_{rraa} or G_{aarr}. These diagrams contain one aa fermion propagator and one aa photon propagator. By flipping labels in G_{rraa} or G_{aarr}, There is always one remaining aa propagator. The bottom row shows a self-energy diagram with vertices constructed from G_{rraa} and G_{aarr} on the left. A possible flipping without aa propagator is shown on the right, which vanishes upon integration of k_0. Multiple soft photon exchanges are allowed on each vertex. Only the outermost one is shown for clarity.

[1] L. Adamczyk *et al.*, Global Λ hyperon polarization in nuclear collisions: evidence for the most vortical fluid, Nature (London) **548**, 62 (2017).

[2] J. Adam *et al.*, Global polarization of Λ hyperons in Au + Au collisions at $\sqrt{s_{NN}} = 200$ GeV, Phys. Rev. C **98**, 014910 (2018).

[3] J. Adam *et al.*, Polarization of Λ ($\bar{\Lambda}$) Hyperons Along the Beam Direction in Au + Au Collisions at $\sqrt{s_{NN}} = 200$ GeV, Phys. Rev. Lett. **123**, 132301 (2019).

[4] D. Kobayashi, T. Yoshikawa, M. Matsuo, R. Iguchi, S. Maekawa, E. Saitoh, and Y. Nozaki, Spin Current Generation Using a Surface Acoustic Wave Generated Via Spin-Rotation Coupling, Phys. Rev. Lett. **119**, 077202 (2017).

[5] M. Matsuo, J. Ieda, K. Harii, E. Saitoh, and S. Maekawa, Mechanical generation of spin current by spin-rotation coupling, Phys. Rev. B **87**, 180402 (2013).

[6] M. A. Metlitski and A. R. Zhitnitsky, Anomalous axion interactions and topological currents in dense matter, Phys. Rev. D **72**, 045011 (2005).

[7] D. T. Son and A. R. Zhitnitsky, Quantum anomalies in dense matter, Phys. Rev. D **70**, 074018 (2004).

[8] J. Erdmenger, M. Haack, M. Kaminski, and A. Yarom, Fluid dynamics of R-charged black holes, J. High Energy Phys. 01 (2009) 055.

[9] N. Banerjee, J. Bhattacharya, S. Bhattacharyya, S. Dutta, R. Loganayagam, and P. Surowka, Hydrodynamics from charged black branes, J. High Energy Phys. 01 (2011) 094.

[10] Y. Neiman and Y. Oz, Relativistic hydrodynamics with general anomalous charges, J. High Energy Phys. 03 (2011) 023.

[11] K. Landsteiner, E. Megias, and F. Pena-Benitez, Gravitational Anomaly and Transport, Phys. Rev. Lett. **107**, 021601 (2011).

[12] K. Hattori, Y. Hidaka, and D.-L. Yang, Axial kinetic theory and spin transport for fermions with arbitrary mass, Phys. Rev. D **100**, 096011 (2019).

[13] N. Weickgenannt, X.-L. Sheng, E. Speranza, Q. Wang, and D. H. Rischke, Kinetic theory for massive spin-1/2 particles from the Wigner-function formalism, Phys. Rev. D **100**, 056018 (2019).

[14] J.-H. Gao and Z.-T. Liang, Relativistic quantum kinetic theory for massive fermions and spin effects, Phys. Rev. D **100**, 056021 (2019).

[15] Y.-C. Liu, K. Mameda, and X.-G. Huang, Covariant spin kinetic theory I: Collisionless limit, Chin. Phys. C **44**, 094101 (2020); **45**, 089001(E) (2021).

[16] X. Guo, Massless limit of transport theory for massive fermions, Chin. Phys. C **44**, 104106 (2020).

[17] D. T. Son and N. Yamamoto, Berry Curvature, Triangle Anomalies, and the Chiral Magnetic Effect in Fermi Liquids, Phys. Rev. Lett. **109**, 181602 (2012).

[18] D. T. Son and N. Yamamoto, Kinetic theory with Berry curvature from quantum field theories, Phys. Rev. D **87**, 085016 (2013).

[19] M. A. Stephanov and Y. Yin, Chiral Kinetic Theory, Phys. Rev. Lett. **109**, 162001 (2012).

[20] S. Pu, J.-h. Gao, and Q. Wang, A consistent description of kinetic equation with triangle anomaly, Phys. Rev. D **83**, 094017 (2011).

[21] J.-W. Chen, S. Pu, Q. Wang, and X.-N. Wang, Berry Curvature and Four-Dimensional Monopoles in the

Relativistic Chiral Kinetic Equation, Phys. Rev. Lett. **110**, 262301 (2013).

[22] Y. Hidaka, S. Pu, and D.-L. Yang, Relativistic chiral kinetic theory from quantum field theories, Phys. Rev. D **95**, 091901 (2017).

[23] C. Manuel and J. M. Torres-Rincon, Kinetic theory of chiral relativistic plasmas and energy density of their gauge collective excitations, Phys. Rev. D **89**, 096002 (2014).

[24] C. Manuel and J. M. Torres-Rincon, Chiral transport equation from the quantum Dirac Hamiltonian and the on-shell effective field theory, Phys. Rev. D **90**, 076007 (2014).

[25] A. Huang, S. Shi, Y. Jiang, J. Liao, and P. Zhuang, Complete and consistent chiral transport from wigner function formalism, Phys. Rev. D **98**, 036010 (2018).

[26] S. Carignano, C. Manuel, and J. M. Torres-Rincon, Consistent relativistic chiral kinetic theory: A derivation from on-shell effective field theory, Phys. Rev. D **98**, 076005 (2018).

[27] J.-H. Gao, Z.-T. Liang, Q. Wang, and X.-N. Wang, Disentangling covariant Wigner functions for chiral fermions, Phys. Rev. D **98**, 036019 (2018).

[28] Z. Wang, X. Guo, S. Shi, and P. Zhuang, Mass correction to chiral kinetic equations, Phys. Rev. D **100**, 014015 (2019).

[29] S. Lin and A. Shukla, Chiral kinetic theory from effective field theory revisited, J. High Energy Phys. 06 (2019) 060.

[30] J.-H. Gao, Z.-T. Liang, and Q. Wang, Dirac sea and chiral anomaly in the quantum kinetic theory, Phys. Rev. D **101**, 096015 (2020).

[31] T. Hayata, Y. Hidaka, and K. Mameda, Second order chiral kinetic theory under gravity and antiparallel charge-energy flow, J. High Energy Phys. 05 (2021) 023.

[32] S.-Z. Yang, J.-H. Gao, Z.-T. Liang, and Q. Wang, Second-order charge currents and stress tensor in a chiral system, Phys. Rev. D **102**, 116024 (2020).

[33] S. Lin and L. Yang, Chiral kinetic theory from Landau level basis, Phys. Rev. D **101**, 034006 (2020).

[34] S. Lin and L. Yang, Magneto-vortical effect in strong magnetic field, J. High Energy Phys. 06 (2021) 054.

[35] X.-L. Luo and J.-H. Gao, Covariant chiral kinetic equation in non-abelian gauge field from “covariant gradient expansion”, J. High Energy Phys. 11 (2021) 115.

[36] J.-j. Zhang, R.-h. Fang, Q. Wang, and X.-N. Wang, A microscopic description for polarization in particle scatterings, Phys. Rev. C **100**, 064904 (2019).

[37] S. Li and H.-U. Yee, Quantum kinetic theory of spin polarization of massive quarks in perturbative QCD: Leading log, Phys. Rev. D **100**, 056022 (2019).

[38] S. Carignano, C. Manuel, and J. M. Torres-Rincon, Chiral kinetic theory from the on-shell effective field theory: Derivation of collision terms, Phys. Rev. D **102**, 016003 (2020).

[39] D.-L. Yang, K. Hattori, and Y. Hidaka, Effective quantum kinetic theory for spin transport of fermions with collsional effects, J. High Energy Phys. 07 (2020) 070.

[40] Z. Wang, X. Guo, and P. Zhuang, Equilibrium spin distribution from detailed balance, Eur. Phys. J. C **81**, 799 (2021).

[41] S. Shi, C. Gale, and S. Jeon, From chiral kinetic theory to relativistic viscous spin hydrodynamics, Phys. Rev. C **103**, 044906 (2021).

[42] N. Weickgenannt, E. Speranza, X.-l. Sheng, Q. Wang, and D. H. Rischke, Generating Spin Polarization from Vorticity through Nonlocal Collisions, Phys. Rev. Lett. **127**, 052301 (2021).

[43] D. Hou and S. Lin, Polarization rotation of chiral fermions in vortical fluid, Phys. Lett. B **818**, 136386 (2021).

[44] N. Yamamoto and D.-L. Yang, Chiral radiation transport theory of neutrinos, Astrophys. J. **895**, 56 (2020).

[45] N. Weickgenannt, E. Speranza, X.-l. Sheng, Q. Wang, and D. H. Rischke, Derivation of the nonlocal collision term in the relativistic Boltzmann equation for massive spin-1/2 particles from quantum field theory, Phys. Rev. D **104**, 016022 (2021).

[46] X.-L. Sheng, N. Weickgenannt, E. Speranza, D. H. Rischke, and Q. Wang, From Kadanoff-Baym to Boltzmann equations for massive spin-1/2 fermions, Phys. Rev. D **104**, 016029 (2021).

[47] Z. Wang and P. Zhuang, Damping and polarization rates in near equilibrium state, arXiv:2105.00915.

[48] W. Florkowski, B. Friman, A. Jaiswal, and E. Speranza, Relativistic fluid dynamics with spin, Phys. Rev. C **97**, 041901 (2018).

[49] D. Montenegro, L. Tinti, and G. Torrieri, Ideal relativistic fluid limit for a medium with polarization, Phys. Rev. D **96**, 056012 (2017); **96**, 079901(A) (2017).

[50] D. Montenegro and G. Torrieri, Causality and dissipation in relativistic polarizable fluids, Phys. Rev. D **100**, 056011 (2019).

[51] K. Hattori, M. Hongo, X.-G. Huang, M. Matsuo, and H. Taya, Fate of spin polarization in a relativistic fluid: An entropy-current analysis, Phys. Lett. B **795**, 100 (2019).

[52] A. D. Gallegos, U. Gürsoy, and A. Yarom, Hydrodynamics of spin currents, SciPost Phys. **11**, 041 (2021).

[53] W. Florkowski, A. Kumar, and R. Ryblewski, Relativistic hydrodynamics for spin-polarized fluids, Prog. Part. Nucl. Phys. **108**, 103709 (2019).

[54] F. Becattini, W. Florkowski, and E. Speranza, Spin tensor and its role in non-equilibrium thermodynamics, Phys. Lett. B **789**, 419 (2019).

[55] S. Bhadury, W. Florkowski, A. Jaiswal, A. Kumar, and R. Ryblewski, Relativistic dissipative spin dynamics in the relaxation time approximation, Phys. Lett. B **814**, 136096 (2021).

[56] K. Fukushima and S. Pu, Spin hydrodynamics and symmetric energy-momentum tensors—A current induced by the spin vorticity–, Phys. Lett. B **817**, 136346 (2021).

[57] S. Li, M. A. Stephanov, and H.-U. Yee, Nondissipative Second-Order Transport, Spin, and Pseudogauge Transformations in Hydrodynamics, Phys. Rev. Lett. **127**, 082302 (2021).

[58] M. Hongo, X.-G. Huang, M. Kaminski, M. Stephanov, and H.-U. Yee, Relativistic spin hydrodynamics with torsion and linear response theory for spin relaxation, J. High Energy Phys. 11 (2021) 150.

[59] H.-H. Peng, J.-J. Zhang, X.-L. Sheng, and Q. Wang, Ideal spin hydrodynamics from Wigner function approach, Chin. Phys. Lett. **38**, 116701 (2021)..

[60] D. She, A. Huang, D. Hou, and J. Liao, Relativistic viscous hydrodynamics with angular momentum, arXiv:2105.04060.

[61] P. B. Arnold, G. D. Moore, and L. G. Yaffe, Effective kinetic theory for high temperature gauge theories, J. High Energy Phys. 01 (2003) 030.

[62] P. B. Arnold, G. D. Moore, and L. G. Yaffe, Transport coefficients in high temperature gauge theories. 1. Leading log results, J. High Energy Phys. 11 (2000) 001.

[63] P. B. Arnold, G. D. Moore, and L. G. Yaffe, Transport coefficients in high temperature gauge theories. 2. Beyond leading log, J. High Energy Phys. 05 (2003) 051.

[64] J.-P. Blaizot and E. Iancu, The quark gluon plasma: Collective dynamics and hard thermal loops, Phys. Rep. **359**, 355 (2002).

[65] K. Hattori, Y. Hidaka, N. Yamamoto, and D.-L. Yang, Wigner functions and quantum kinetic theory of polarized photons, J. High Energy Phys. 02 (2021) 001.

[66] X.-G. Huang, P. Mitkin, A. V. Sadofyev, and E. Speranza, Zilch vortical effect, berry phase, and kinetic theory, J. High Energy Phys. 10 (2020) 117.

[67] X.-G. Huang and A. V. Sadofyev, Chiral vortical effect for an arbitrary spin, J. High Energy Phys. 03 (2019) 084.

[68] S. Mrowczynski, Color filamentation in ultrarelativistic heavy ion collisions, Phys. Lett. B **393**, 26 (1997).

[69] S. Mrowczynski, B. Schenke, and M. Strickland, Color instabilities in the quark–gluon plasma, Phys. Rep. **682**, 1 (2017).

[70] P. Romatschke and M. Strickland, Collective modes of an anisotropic quark gluon plasma, Phys. Rev. D **68**, 036004 (2003).

[71] P. B. Arnold, D. Son, and L. G. Yaffe, The Hot baryon violation rate is $O(\alpha_{\mathrm{w}}^5 T^4)$, Phys. Rev. D **55**, 6264 (1997).

[72] E. Petitgirard, Massive fermion dispersion relation at finite temperature, Z. Phys. C **54**, 673 (1992).

[73] P. B. Arnold, G. D. Moore, and L. G. Yaffe, Photon emission from ultrarelativistic plasmas, J. High Energy Phys. 11 (2001) 057.

[74] Y. Hidaka, S. Pu, and D.-L. Yang, Nonlinear responses of chiral fluids from kinetic theory, Phys. Rev. D **97**, 016004 (2018).

[75] J.-Y. Chen, D. T. Son, M. A. Stephanov, H.-U. Yee, and Y. Yin, Lorentz Invariance in Chiral Kinetic Theory, Phys. Rev. Lett. **113**, 182302 (2014).

[76] J.-Y. Chen, D. T. Son, and M. A. Stephanov, Collisions in Chiral Kinetic Theory, Phys. Rev. Lett. **115**, 021601 (2015).

[77] S. Y. F. Liu and Y. Yin, Spin polarization induced by the hydrodynamic gradients, J. High Energy Phys. 07 (2021) 188.

[78] J.-h. Gao, J.-Y. Pang, and Q. Wang, Chiral vortical effect in Wigner function approach, Phys. Rev. D **100**, 016008 (2019).

[79] F. Becattini, V. Chandra, L. Del Zanna, and E. Grossi, Relativistic distribution function for particles with spin at local thermodynamical equilibrium, Ann. Phys. (Amsterdam) **338**, 32 (2013).

[80] M. Le Bellac, *Thermal Field Theory*, Cambridge Monographs on Mathematical Physics (Cambridge University Press, Cambridge, England, 2011).

[81] E. Wang and U. W. Heinz, A generalized fluctuation dissipation theorem for nonlinear response functions, Phys. Rev. D **66**, 025008 (2002).